The Journal of Immunology

Inducible TAP1 Negatively Regulates the Antiviral Innate Immune Response by Targeting the TAK1 Complex

Zhangchuan Xia, Gang Xu, Xiaodan Yang, Nanfang Peng, Qi Zuo, Shengli Zhu, Hua Hao, Shi Liu and Ying Zhu

J Immunol 2017; 198:3690-3704; Prepublished online 29 March 2017;
doi: 10.4049/jimmunol.1601588
http://www.jimmunol.org/content/198/9/3690

The Journal of Immunology is published twice each month by
The American Association of Immunologists, Inc.,
1451 Rockville Pike, Suite 650, Rockville, MD 20852

Print ISSN: 0022-1767 Online ISSN: 1550-6606.

Inducible TAP1 Negatively Regulates the Antiviral Innate Immune Response by Targeting the TAK1 Complex

Zhangchuan Xia, Gang Xu, Xiaodan Yang, Nanfang Peng, Qi Zuo, Shengli Zhu, Hua Hao, Shi Liu, and Ying Zhu

The innate immune response is critical for host defense and must be tightly controlled, but the molecular mechanisms responsible for its negative regulation are not yet completely understood. In this study, we report that transporter 1, ATP-binding cassette, subfamily B (TAP1), a virus-inducible endoplasmic reticulum–associated protein, negatively regulated the virus-triggered immune response. In this study, we observed upregulated expression of TAP1 following virus infection in human lung epithelial cells (A549), THP-1 monocytes, HeLa cells, and Vero cells. The overexpression of TAP1 enhanced virus replication by inhibiting the virus-triggered activation of NF-κB signaling and the production of IFNs, IFN-stimulated genes, and proinflammatory cytokines. TAP1 depletion had the opposite effect. In response to virus infection, TAP1 interacted with the TGF-β–activated kinase (TAK)1 complex and impaired the phosphorylation of TAK1, subsequently suppressing the phosphorylation of the IκB kinase complex and NF-κB inhibitor α (IκBα) as well as NF-κB nuclear translocation. Our findings collectively suggest that TAP1 plays a novel role in the negative regulation of virus-triggered NF-κB signaling and the innate immune response by targeting the TAK1 complex. ***The Journal of Immunology*****, 2017, 198: 3690–3704.**

The innate immune system serves as the first line of host defense against virus infections. Upon virus infection, structurally conserved viral components called pathogen-associated molecular patterns are recognized by pattern-recognition receptors (PRRs) in the cell. The main PRRs include the TLRs and retinoic acid–inducible gene-I (RIG-I)–like receptors (RLRs) (1). TLRs are transmembrane receptors that sense various ligands. For example, TLR3, TLR7, and TLR9 are responsible for the detection of viral dsRNA, ssRNA, and DNA, respectively (2, 3). RLRs such as RIG-I and melanoma differentiation-associated protein 5 are cytosolic sensors of intracellular viral RNA (vRNA) (4). Most virus-triggered signaling pathways are dependent on IFN regulatory factor (IRF)3/7 and NF-κB activation, which induces the production of a series of IFNs and proinflammatory cytokines (5). The IFNs subsequently bind to cognate receptors on the surface of the surrounding cells to activate the Jak/STAT pathway, which results in the transcription of a wide range of IFN-stimulated genes (ISGs), including protein kinase R (PKR), myxovirus resistance 1 (Mx1), and 2′-5′-oligoadenylate synthetase 1 (OAS1) (6, 7). These cytokines and downstream effecters act to limit viral replication, eradicate virus-infected cells, and facilitate the initiation of the adaptive immune response (8–11).

Upon ligand binding, the TLRs dimerize and interact with the adapter protein Myd88 or Toll/IL-1R domain–containing adapter inducing IFN-β (TRIF) (12), which recruits IRAK family members and TNFR-associated factor (TRAF)6. Activated TRAF6 synthesizes lysine 63–linked polyubiquitin chains on itself and other proteins, which then serve as a scaffold to recruit the TGF-β–activated protein kinase (TAK)1–TAK1-binding protein (TAB) 2–TAB3 complex, which results in the activation of TAK1 (13, 14). Activated TAK1 then phosphorylates the IκB kinase (IKK) complex and IκBα, leading to activation of NF-κB (12, 15). The IRF family is also activated. TBK1 is essential for both IRF3 and IRF7 phosphorylation (16–18), and other molecules such as Myd88 and TRAF6 are also involved (19, 20). In contrast, activation of RLRs such as RIG-I and melanoma differentiation-associated protein 5 by dsRNAs or certain viruses leads to recruitment of the mitochondrial antiviral signaling protein (MAVS; also called VISA, IPS-1, and Cardif) (4, 21–23). MAVS contains multiple TRAF-interacting motifs, which interact with TRAF family members to activate downstream molecules. Similar to the TLR signaling, TAK1 plays a critical role in NF-κB activation, and IRF3 is directly activated by TBK1/IKKε (24, 25). NF-κB activation is an important common event in these signaling pathways and requires the signal-induced phosphorylation and degradation of IκB proteins (26). The kinase that phosphorylates IκB, termed the IKK complex, consists of two catalytic subunits, IKKα and IKKβ, and one regulatory subunit NEMO (also known

State Key Laboratory of Virology, College of Life Sciences, Wuhan University, Wuhan 430072, China

ORCID: 0000-0002-4451-8456 (G.X.).

Received for publication September 12, 2016. Accepted for publication March 3, 2017.

This work was supported by Major State Basic Research Development Program of China Grant 2013CB911102 and by National Natural Science Foundation of China Grants 81461130019, 81271821, and 31570870. The funding agencies had no role in study design, data collection or analysis, decision to publish, or preparation of the manuscript.

Address correspondence and reprint requests to Prof. Ying Zhu, State Key Laboratory of Virology, College of Life Sciences, Wuhan University, Wuhan 430072, China. E-mail address: yingzhu@whu.edu.cn

The online version of this article contains supplemental material.

Abbreviations used in this article: eGFP, enhanced GFP; ER, endoplasmic reticulum; EV71, enterovirus 71; HA, hemagglutinin; IAV, influenza A virus; IKK, IκB kinase; IRF, IFN regulatory factor; ISG, IFN-stimulated gene; ISRE, IFN-stimulated response element; KO, knockout; MAVS, mitochondrial antiviral signaling protein; MHC I, MHC class I; MOI, multiplicity of infection; Mx1, myxovirus resistance 1; NP, nucleoprotein; OAS1, 2′-5′-oligoadenylate synthetase 1; PEI, polyethyleneimine; PKR, protein kinase R; PRR, pattern recognition receptor; qRT-PCR, quantitative real-time RT-PCR; RIG-I, retinoic acid–inducible gene-I; RLR, retinoic acid–inducible gene-I–like receptor; RNAi, RNA interference; SeV, Sendai virus; sh, short hairpin; siRNA, small interfering RNA; TAB, TGF-β–activated protein kinase 1–binding protein; TAK, TGF-β–activated protein kinase; TAP1, transporter 1, ATP-binding cassette, subfamily B; TRAF, TNFR-associated factor; TRIF, Toll/IL-1R domain–containing adapter inducing IFN-β; vRNA, viral RNA; VSV, vesicular stomatitis virus.

as IKK-γ) (2, 27). Notably, the TAK1 protein kinase complex, which phosphorylates and activates the IKK complex, is composed of the TAK1 binding partners, TAB1, TAB2, or TAB3, which are required for TAK1 kinase activity (28, 29).

Transporter 1, ATP-binding cassette, subfamily B (TAP1) is a member of the MDR/TAP subfamily of ATP-binding cassette transporters. The 75-kDa TAP1 protein, together with TAP2, forms the TAP complex, which resides on the endoplasmic reticulum (ER) membrane and is responsible for the pumping of degraded cytosolic antigenic peptides across the ER into the membrane-bound compartment for association with MHC class I (MHC I) molecules (30–32). Antigenic peptides are primarily generated by proteasomal degradation and translocated into the lumen of the ER by the TAP. In the ER, peptides are loaded onto the MHC I molecules in a process orchestrated by a multisubunit peptide-loading complex. Peptide–MHC I complexes are anchored to the cell surface for Ag presentation to cytotoxic T cells, which eventually leads to the elimination of virally infected or malignantly transformed cells (33). Certain viruses employ viral proteins to inhibit TAP function or downregulate TAP expression to evade the immune response, such as the HSV I protein ICP47 and the human CMV protein US6 (34, 35). The structural and functional dissection of the human CMV protein US6 was previously reported (36). Recently, the cryo-electron microscopic structure of human TAP in a complex with its inhibitor ICP47, a small protein produced by the HSV-1, was also reported (37). Additionally, investigators have observed reduced levels of TAP expression in various types of tumors, which is thought to be one mechanism for tumor immune evasion (38).

Several functions of TAP1 have been described, which have mainly focused on Ag presentation and adaptive immunity. However, its role in innate immune signaling in response to viral infection has never been established. In this study, we demonstrated that TAP1 was induced after virus infection and enhanced the replication of influenza A virus (IAV), vesicular stomatitis virus (VSV), and human enterovirus 71 (EV71). Furthermore, TAP1 constrains NF-κB signaling and the innate antiviral response by targeting the TAK1–TAB complex and blocking TAK1 phosphorylation. Thus, our results describe a previously unrecognized role of TAP1 as a virus-inducible negative regulator of innate immunity.

Materials and Methods

Cells and viruses

Human lung epithelial cells (A549) were cultured in F12K medium. HEK293T, HeLa, and Vero cells were cultured in DMEM. Human embryonic RD cells were cultured in MEM. Human THP-1 monocytes were cultured in RPMI 1640 medium. All media were supplemented with 10% heat-inactivated FBS, 100 U/ml penicillin, and 100 mg/ml streptomycin sulfate, and all cell cultures were maintained at 37°C in a 5% CO_2 incubator. All of the cell lines above were purchased from American Type Culture Collection. The influenza virus A/Hong Kong/498/97 (H3N2) strain and the Indiana serotype of VSV were provided by the China Center for Type Culture Collection. A recombinant VSV carrying the enhanced GFP (eGFP) gene (VSV-eGFP) and the EV71 strain were described previously (39, 40).

Antibodies

Abs against human TAP1 (11114-1-AP), STAT1 (10144-2-AP), Mx1 (13750-1-AP), TAK1 (12330-2-AP), NF-κB p50 (14220-1-AP), IRF7 (22392-1-AP), β-actin (60008-1-Ig), β-tubulin (66249-1-Ig), and EV71 VP1 were purchased from the ProteinTech Group (Wuhan, China). Abs against PKR (sc-100378), OAS1 (sc-98424), TAK1 (sc-7967), NF-κB p65 (sc-372), IRF3 (sc-9082), LaminA (sc-20680), TRAF6 (sc-7221), IKKα/β (sc-7607), and GRP78 (sc-1050) were purchased from Santa Cruz Biotechnology (Santa Cruz, CA). Abs against TAP1 (12341S), p-IKK (2697S), IκBα (4812S), p-IκBα (2859S), p-TAK1 (4508S), p38 MAPK (8690S), and p-p38 MAPK (4511S) were purchased from Cell Signaling Technology (Beverly, MA). Abs against Flag (M185-3L) and hemagglutinin (HA; M180-3) were purchased from Medical and Biological Laboratories (Nagoya, Japan). The Ab against GAPDH (cw0100A) was purchased from CoWin Biotech (Beijing, China).

Plasmids and small interfering RNA

The coding regions of human TAP1 were amplified by PCR, digested with BamHI/XhoI, EcoRI/XbaI, or BamHI/EcoRI, and cloned directly into the pCMV-tag2B, or pCMV-14-3×Flag, or PKH3-3×HA mammalian expression vectors, respectively, to generate TAP1 expression plasmids. The *TAP1* promoter region (−2000 to +155) was inserted into the XhoI and HindIII sites of pGL3-basic (Promega, Madison, WI) to generate p*TAP1*–Luc. Expression plasmids for Flag-tagged IRAK4, TAK1, TAB1, IKKα, and IκBα and HA-tagged TAK1 and TAB1 were also constructed for this study. All primers used for construction are listed in Supplemental Table I. The TRIF, TBK1, TAB2, TAB3, IKKβ, p50, and p65 overexpression plasmids were previously cloned in our laboratory. Luciferase reporter plasmids for *IFN-λ1*, *IL-6*, and *IL-8* and the expression plasmids for Flag-tagged MAVS and HA-tagged TRAF6 were reported previously (41, 42). The *IFN-β*, IFN-stimulated response element (*ISRE*), and *NF-κB* luciferase reporter plasmids and the Flag-tagged RIG-I expression plasmid were provided by Prof. Hongbing Shu (Wuhan University). Four plasmids involved in producing recombinant lentivirus, namely the two lentiviral vectors pLKO.1-TRC and pLKO.1-scramble short hairpin (sh) RNA and two packaging plasmids (psPAX2 and pMD2.G), were provided by Prof. Yingliang Wu (Wuhan University). To construct the TAP1 RNA interference (RNAi) plasmids, four oligonucleotide pairs were synthesized, annealed, and cloned into the AgeI and BamHI sites of the pLKO.1-TRC vector. The following sequences were targeted for *TAP1* mRNA: no. 1, 5′-CGGGATCTATAACAACACCAT-3′; no. 2, 5′-CCGTGTGTACTTATCC-TGGAT-3′; and no. 3, 5′-CGATACCTTCACTCGAAACTT-3′. All constructs and gifted plasmids were confirmed by DNA sequencing. The specific small interfering RNAs (siRNAs) and irrelevant control siRNA were purchased from RiboBio (Guangzhou, China) with the following sequences: si-*STAT1*, 5′-CUGGAAGAUUUACAAGAUGAA-3′; si-*TAP1*, 5′-CGGGAUCUAUAACAACACCAU-3′.

Generation of stable TAP1-knockdown cells

The lentiviral vector pLKO.1-scramble shRNA or pLKO.1-TAP1 shRNA no. 1, along with lentivirus packaging plasmids psPAX2 and pMD2.G, was cotransfected into HEK293T cells at a ratio of 3:2:2 using polyethyleneimine (PEI; Sigma-Aldrich). After 24 h, the culture medium was replaced with fresh medium. The viruses in the conditioned medium were harvested on 2 consecutive days and filtered with low-protein-binding filters (Millex-HV, 0.45-μm polyvinylidene difluoride; EMD Millipore) before they were aliquoted and stored at −80°C. The cells of interest were seeded into 35-mm cell culture dishes. When the cells were 70% confluent, they were incubated in fresh media containing 8 μg/ml Polybrene, and either 0.1 ml of pLKO.1-scramble shRNA or pLKO.1-TAP1 shRNA no. 1 lentivirus was added. After 24 h, the virus-infected cells were selected for at least 3 d using puromycin (0.8 μg/ml for A549 cells and 1.0 μg/ml for THP-1 monocytes) and then subjected to the required assays.

Generation of IFNAR1knockout cell lines using the CRISPR-Cas9 system

The lentiCRISPR v2 plasmid was a gift of Jianguo Wu (Wuhan University). The specific oligonucleotides targeting the IFNAR1 gene was designed using the Cas9 target design tools (http://www.genome-engineering.org). The following oligonucleotides were used: oligonucleotide 1, 5′-CACC-GACCCTAGTGCTCGTCGCCG-3′ and oligonucleotide 2, 5′-AAAC-CGGCGACGAGCACTAGGGTC-3′. The target guide sequence cloning protocol can be found at the Zhang Laboratory GeCKO Web site (http://www.genome-engineering.org/gecko/). The IFNAR1-specific lentiCRISPR v2 plasmid, lentivirus packaging plasmid psPAX2, and envelope plasmid pMD2.G were cotransfected into HEK293T cells using PEI (Sigma-Aldrich). After 24 h, the culture medium was replaced with fresh medium. The viruses in the conditioned medium were harvested on 2 consecutive days and filtered with low-protein-binding filters (Millex-HV, 0.45-μm polyvinylidene difluoride; EMB Millipore) before they were aliquoted and stored at −80°C. The cells of interest were seeded into six-well plates (4×10^5 cells per well). When the cells were ∼70% confluent, they were incubated in fresh culture medium containing 8 μg/ml Polybrene. The IFNAR1-specific lentiCRISPR v2 lentivirus-containing media or the empty vector lentiCRISPR v2 lentivirus-containing media were added to the cells. After 24 h, the virus-infected cells were selected for

72 h using puromycin (0.8 μg/ml for A549 cells and 2.5 μg/ml for Huh7 cells). Cells that survived were plated at a density of 2000 per well in the A1 well of 96-well plates, and the rest of the wells were added at 100 μl per well fresh culture media. A total of 100 μl of medium of A1 well was transferred to B1 well. After blending, a 1:2 dilution ratio to the last well (H1) of this column was repeated, and 100 μl of medium was removed from H1 well to keep the same volume with the other wells. Then, 100 μl of medium of the first column (A1-H1) was transferred to the second column (A2-H2), and a 1:2 dilution ratio to the last column was repeated (A12-H12). A total of 100 μl of medium was removed from the last column as well. At last, 100 μl of fresh culture medium was added into each well, and cells were cultured until the monoclonal cells were singled out for enlarged culture. The IFNAR1-knockout (KO) cell lines were obtained from these enlarged monoclonal cells and confirmed by immunoblotting.

Measurement of IAV replication

A549 cells were infected with IAV/Hong Kong/498/97 (H3N2) at a multiplicity of infection (MOI) of 1. The viral titers were measured using hemagglutination assays in U-shaped plates, as described previously (43, 44). The relative RNA levels of nucleoprotein (NP)-mRNA, NP-cRNA, and NP-vRNA were determined using quantitative real-time RT-PCR (qRT-PCR) as previously described (44). The following primers were used for the reverse transcription: *NP-vRNA*, 5′-CTCACCGAGTGACATCAA-CATCATG-3′; *NP-cRNA*, 5′-AGTAGAAACAAGGGTATTTTTC-3′; and *NP-mRNA*, oligo(dT). The following primers were used for qRT-PCR: *NP*, 5′-ATCAGACCGAACGAGAATCCAGC-3′ (sense) and 5′-GGAGGCC-CTCTGTTGATTAGTGT-3′ (antisense).

VSV plaque assay

The cells were grown in 12-well plates, transfected with the indicated plasmids for 24 h, and then infected with VSV (MOI of 1). After 1 h, the cells were washed with warm PBS, and fresh medium was added. After 24 h, the supernatants were harvested, diluted to 10^{-6}, 10^{-5}, 10^{-4}, 10^{-3}, and 10^{-2}, and used to infect confluent Vero cells cultured on 24-well plates. At 1 h postinfection, the supernatants were removed, and a mixture of warm 3% low melting point agarose and fresh medium were overlaid. At 72 h postinfection, the cells were stained with 0.2% crystal violet for 2 h, and the overlay was removed. The numbers of plaques were counted, averaged, and multiplied by the dilution factor to determine the viral titer (PFU/ml).

Transient transfection and luciferase reporter assay

A549, RD, Vero, and HeLa cells were transfected using Lipofectamine 2000 (Invitrogen, Carlsbad, CA). HEK293T cells were transfected using PEI (Sigma-Aldrich). For the reporter assay, A549 cells were cotransfected with the luciferase reporter plasmid and the relevant recombinant expression plasmids at an appropriate ratio. A *Renilla* luciferase reporter vector pRL-TK was used as internal control. The reporter gene activities were measured using a Dual-Luciferase reporter assay (Promega), according to the manufacturer's instructions. All reporter assays were repeated at least three times. The data shown are the average values ± SD from one representative experiment.

qRT-PCR

The total RNA was isolated using TRIzol reagent (Invitrogen). The cellular RNA samples were reverse transcribed with random primers, and quantitative PCR assays were performed using an ABI StepOne real-time PCR system (Applied Biosystems) and SYBR RT-PCR kits (Applied Biosystems). The data are shown as the relative abundance of the indicated mRNA normalized to that of GAPDH. All of the primers used for qRT-PCR are listed in Supplemental Table II.

Semiquantitative RT-PCR

The total RNA was isolated and 1 μg of RNA was reverse transcribed with random primers followed by PCR amplification. The PCR products were electrophoresed on a 2.5% agarose gel containing ethidium bromide and visualized by UV light. The PCR primers for the indicated genes were the same as those used in the qRT-PCR experiments.

Coimmunoprecipitation and immunoblot analysis

HEK293T cells (6×10^6), A549 cells, or THP-1 cells (4×10^7) were lysed in 1 ml of lysis buffer (20 mM Tris-HCl [pH 7.4–7.5], 150 mM NaCl, 1 mM EDTA, and 1% [v/v] Nonidet P-40) supplemented with 0.1% of a protease inhibitor mixture. Coimmunoprecipitation and immunoblot analysis were performed as previously described (45).

Subcellular fractionation

A549 cells (4×10^7) were washed with ice-cold PBS, suspended in 1 ml of homogenization buffer (10 mM Tris-HCl [pH 7.4], 2 mM $MgCl_2$, 10 mM KCl, and 250 mM sucrose), and homogenized in a prechilled Dounce homogenizer (Kontes). The homogenate was centrifuged at 5000 × *g* for 10 min to remove the nuclei, mitochondria, and intact cells. The supernatant was further centrifuged at 50,000 × *g* for 30 min to separate the ER-associated membrane fractions (P50K) from the cytosol (S50K). The various fractions were then lysed and subjected to immunoblot analysis.

Nuclear extraction

A549 cells (5×10^6) were washed with ice-cold PBS, collected by centrifugation, and resuspended in hypotonic buffer A (10 mM Tris-HCl [pH 7.4], 5 mM $MgCl_2$, 10 mM NaCl, 1 mM DTT, 10% protease inhibitor mixture) for 15 min on ice prior to incubation with 0.5% Nonidet P-40 on ice for 1 min. The nuclei were pelleted by centrifugation at 13,000 × *g* for 1 min, and the cytosolic protein–containing supernatants were collected. The nuclei in the pellets were resuspended in buffer B (20 mM HEPES-KOH [pH 7.9], 1.5 mM $MgCl_2$, 0.5 mM NaCl, 1 mM DTT, 0.2 mM EDTA, 1% Nonidet P-40, 10% protease inhibitor mixture), vortexed for 15 s, and incubated on ice for 10 min. After three repetitions of the vortex-incubation process and centrifugation at 13,000 × *g* for 30 min, the nuclear protein–containing supernatants were collected. The indicated proteins were detected using immunoblot analysis.

Confocal immunofluorescence

A549 cells were fixed with 4% paraformaldehyde for 10 min at room temperature, permeabilized with PBS containing 0.1% Triton X-100 on ice for 20 min, and blocked with PBS containing 4% BSA for 1 h at room temperature. Then, the cells were immunostained with the indicated primary Abs overnight at 4°C followed by incubation with the relevant dye-conjugated secondary Abs (ProteinTech Group) at 37°C for 1 h. The nuclei were stained with DAPI (Vector Laboratories) for 5 min at 37°C. Images were acquired using an Olympus laser scanning confocal microscope.

Statistical analysis

All experiments were repeated at least three times with similar results. Representative data are shown. The statistical analyses were performed using paired Student *t* tests. A p value <0.05 was considered statistically significant.

Results

TAP1 expression is upregulated during virus infection

To investigate the TAP1 expression level during a viral infection, A549 cells were infected with IAV (MOI of 1) for the indicated times. The results showed that TAP1 expression at both the mRNA and protein levels was clearly upregulated by IAV in a time-dependent manner as determined by qRT-PCR and immunoblotting (Fig. 1A). In THP-1 monocytes, a human immune cell line, TAP1 expression was also induced at the mRNA level following infection with either IAV or VSV (Fig. 1B). Additionally, we found increased expression of TAP1 in HeLa cells following Sendai virus (SeV) infection (Fig. 1C). Moreover, analysis of the function of the *TAP1* promoter (−2000 to +155) was performed using a luciferase reporter assay in virus-infected A549 cells. The results showed that IAV (Fig. 1D, left) and SeV (Fig. 1D, right) significantly induced the TAP1 promoter activity. These data collectively demonstrated that TAP1 expression is inducible during virus infection. Because previous studies reported that TAP1 is induced by IFNs and some TLR ligands in a cell type–specific manner (46–49), it would be interesting to see whether the induction of TAP1 in this infection system was due to the virus-induced IFNs or the virus itself. We used STAT1-specific siRNA to knock down the endogenous STAT1 expression in A549 cells, and the results showed that TAP1 expression was still significantly upregulated by IAV at both the mRNA and protein levels (Fig. 1E). Consistently, we found that SeV could induce TAP1 mRNA expression in the Vero cell line, which lacks functional type I IFN

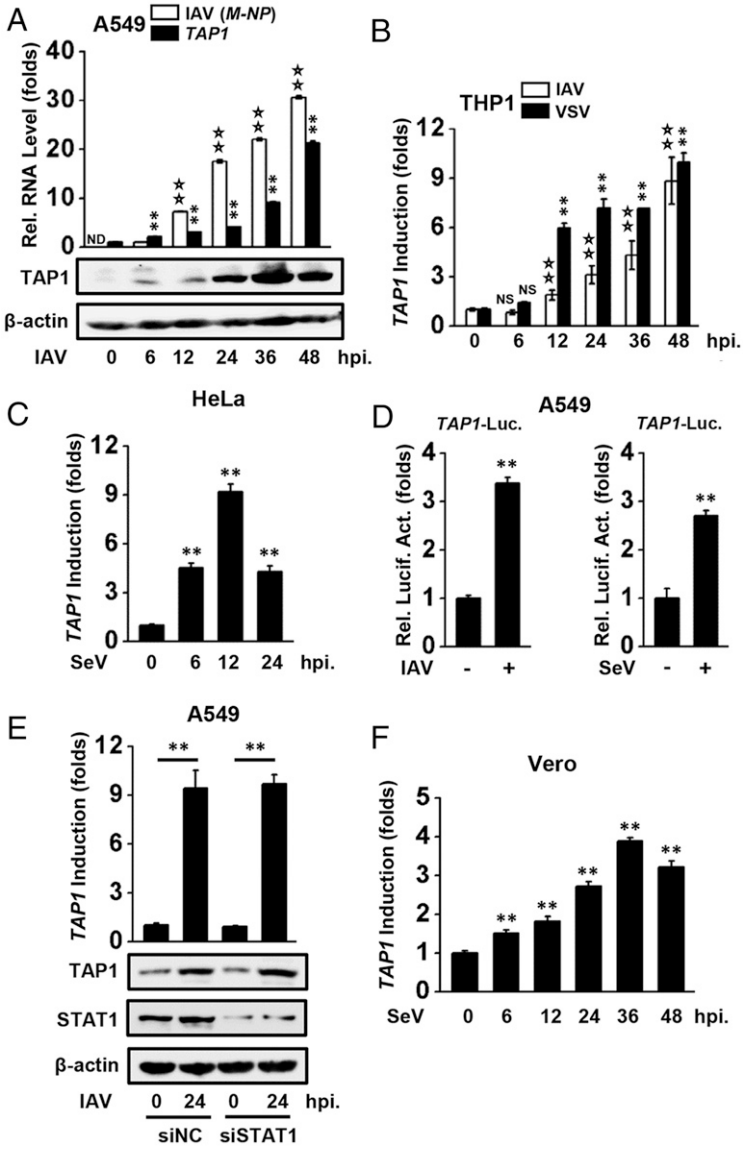

FIGURE 1. Virus infection upregulates TAP1 expression. (**A**) A549 cells were infected with H3N2 at an MOI of 1 for the indicated times. The levels of IAV RNA and TAP1 mRNA were determined by qRT-PCR, and the protein levels of TAP1 were determined by immunoblotting. (**B**) THP-1 cells were infected with H3N2 or VSV at an MOI of 1 for the indicated times. The TAP1 mRNA levels were determined by qRT-PCR. (**C**) HeLa cells were infected with SeV at an MOI of 1 for the indicated times. The TAP1 mRNA levels were determined by qRT-PCR. (**D**) A549 cells were transfected with luciferase reporter plasmids containing the *TAP1* promoter (−2000 to +155). pRL-TK was cotransfected as an internal control. At 24 h posttransfection, the cells were mock infected or infected with H3N2 or SeV at an MOI of 1 for 12 h, followed by the reporter assay. (**E**) A549 cells were transfected with the STAT1-specific siRNA or nonsense control siRNA for 24 h before infection with H3N2 (MOI of 1) for another 24 h. The mRNA levels of TAP1 were determined by qRT-PCR, and the protein levels of TAP1 and STAT1 were determined by immunoblotting. (**F**) Vero cells were infected with SeV at an MOI of 1 for the indicated times. The TAP1 mRNA levels were determined by qRT-PCR. The graphs show the means ± SD, $n = 3$. $^{**}p < 0.01$. ND, not detected.

genes (50, 51). Taken together, these data suggested that the upregulation of TAP1 in this system is not dependent on IFNs.

TAP1 constrains the cellular antiviral response

The finding that TAP1 was a virus-induced host factor prompted us to explore whether TAP1 influenced the cellular antiviral activity. Infection with various viruses, including IAV, VSV, and EV71, was used to assess the role of TAP1 in the antiviral response. The reason we experimented with multiple viral infection systems was to test whether our observations had broad implications. IAV replication experiments showed that TAP1 overexpression significantly increased the IAV NP gene RNA levels including mRNA, cRNA, and vRNA in A549 cells (Fig. 2A). In a VSV plaque assay, we observed a higher viral titer in the TAP1-transfected A549 cells than in the control cells (Fig. 2B). Furthermore, TAP1 facilitated the replication of the recombinant VSV-eGFP virus in A549 cells, which was determined by measuring eGFP expression by flow cytometry and was visualized by fluorescence microscopy (Fig. 2C). Subsequently, we examined the effect of TAP1 on EV71 replication. TAP1 overexpression significantly increased the number of copies of EV71 in the supernatant of the RD cells (Fig. 2D, left) as determined by qRT-PCR using an EV71 VP1 expression plasmid as a standard (40). The expression levels of the intracellular vRNA and the VP1 protein, which is one of the major components of EV71 capsid, were also enhanced in the cells in which TAP1 was overexpressed (Fig. 2D, right). To explore the function of the endogenous TAP1 protein, we constructed three RNAi plasmids (pLKO.1-shTAP1 nos. 1, 2, and 3) that targeted the TAP1 mRNA. The results showed that pLKO.1-shTAP1 no. 1 displayed the highest knockdown efficiency for both endogenous (Fig. 2E, left) and overexpressed TAP1 (Fig. 2E, right). Therefore, this plasmid was used for the subsequent transient RNAi transfections as well as to establish stable TAP1-knockdown A549 and THP-1 cells. In the virus replication experiments, TAP1 knockdown clearly impaired IAV (Fig. 2F) and EV71 (Fig. 2G) multiplication, which was consistent with the results using the overexpression approach. To further confirm that the TAP1 depletion was responsible for the impaired virus replication, we generated stable TAP1-knockdown A549 cells and examined the knockdown efficiency (Fig. 2H). The IAV replication was inhibited in the TAP1-KD cells compared with the control scramble-KD cells and was fully rescued when TAP1 was restored by ectopically overexpressing TAP1 in the TAP1-KD cells (Fig. 2I). Thus, we demonstrated that TAP1 had a universal function of promoting virus replication. We therefore wondered whether the mechanisms behind these events were linked to the

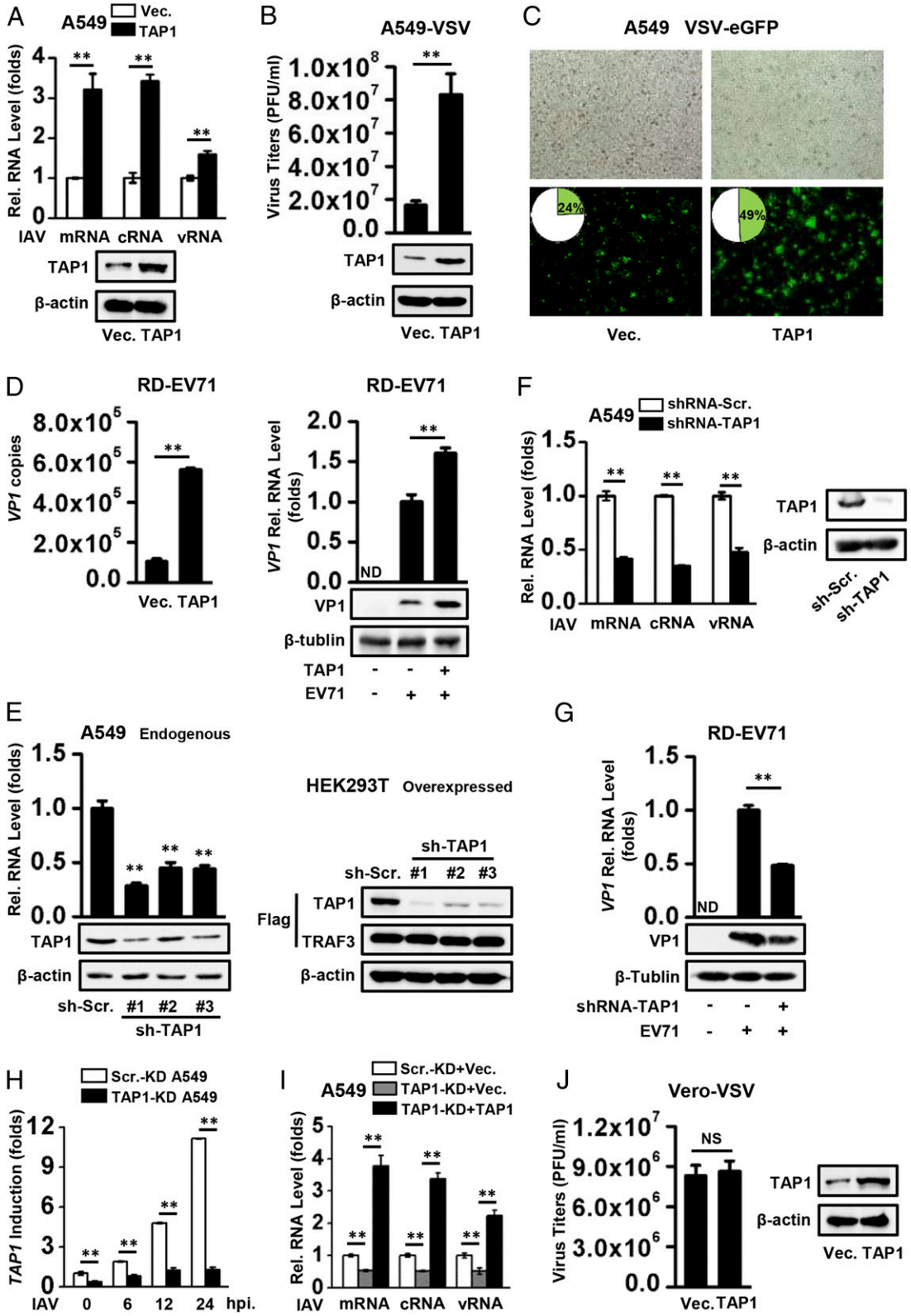

FIGURE 2. TAP1 negatively regulates the cellular antiviral response. (**A**) A549 cells were transfected with the vector or TAP1 expression plasmids for 24 h and then infected with IAV (MOI of 1) for another 24 h. The relative levels of NP-specific mRNA, cRNA, and vRNA were measured using qRT-PCR. The TAP1 protein level was analyzed using immunoblotting. (**B**) A549 cells were transfected with the vector or TAP1 expression plasmids for 24 h and infected with VSV (MOI of 1). At 24 h postinfection, the supernatants were harvested and analyzed for VSV production using a standard plaque assay. The cells were lysed and the TAP1 protein was analyzed using immunoblotting. (**C**) A549 cells were transfected with the vector or TAP1 expression plasmids for 24 h and then infected with VSV-eGFP (MOI of 1) for 7 h. The VSV-eGFP replication was measured by flow cytometry for eGFP expression (data shown in insets) and was visualized by fluorescence microscopy. Original magnification ×10. (**D**) RD cells were transfected with the vector or TAP1 expression plasmids for 24 h and incubated with 1 MOI of enterovirus71. After 1 h, the cells were washed with warm PBS, and fresh medium was added. At 24 h postinfection, the number of EV71 copies in the supernatants of RD cells was determined using qRT-PCR (left panel). The intracellular levels of the vRNA and VP1 protein were determined using qRT-PCR and immunoblotting (right panel). (**E**) Interfering effects of pLKO.1-TAP1 (*Figure legend continues*)

host innate immune response. We tested the effect of TAP1 on VSV replication in the Vero cell line, which lacks functional type I IFN genes (50, 51). The result indicated that VSV replication was not affected by TAP1 in Vero cells (Fig. 2J), which implied that the function of TAP1 in the promotion of virus replication may be associated with IFN signaling.

TAP1 suppressed virus-triggered expression of IFNs and ISGs

To explore the potential role of the TAP1 protein in the virus-triggered innate immune signaling pathway, we performed reporter assays in A549 cells infected with SeV (MOI of 1). In these reporter assays, overexpression of TAP1 inhibited the SeV-induced activation of the *IFN-β* and *IFN-λ1* promoters (Fig. 3A). Because activation of the IFN promoters requires recruitment of the transcription factors IRFs or NF-κB to the corresponding binding sites, we further assessed the effect of TAP1 on the *ISRE* and *NF-κB* reporter luciferase activity. Interestingly, the expression of TAP1 led to a reduced SeV stimulation-induced activation of the *NF-κB* reporter luciferase activity but not that of *ISRE* (Fig. 3A), which indicated that TAP1 only affected the NF-κB signaling. Furthermore, overexpression of TAP1 inhibited the SeV-triggered expression of IFN-α, IFN-β, and IFN-λ1 at the mRNA level, as measured by qRT-PCR (Fig. 3B) and semiquantitative RT-PCR (Fig. 3C). Subsequently, we detected the expression of the ISGs, including Mx1, PKR, and OAS1, using qRT-PCR and immunoblotting. The results indicated that TAP1 significantly decreased the mRNA (Fig. 3D) and protein (Fig. 3E) levels of Mx1, PKR, and OAS1. Collectively, these data suggested that TAP1 inhibited the virus-triggered induction of the IFNs and ISGs.

Knockdown of TAP1 enhances virus-triggered expression of IFNs and ISGs

We next investigated whether endogenous TAP1 functioned as a negative regulator of innate immune signaling. A549 cells were transiently transfected with shTAP1 and the indicated reporter plasmids. The reporter assays showed that knockdown of TAP1 enhanced the SeV-triggered activation of the *IFN-β* and *IFN-λ1* promoters and the *NF-κB* reporter luciferase activity (Fig. 4A). To further verify the role of the endogenous TAP1, we constructed stable TAP1-knockdown A549 and THP1 cells using a lentiviral system. As shown by immunoblotting, the TAP1 expression was significantly reduced in the TAP1-knockdown cells relative to scramble-knockdown cells, and the reduced level was partially restored during virus infection (Fig. 4B). Moreover, the stable TAP1-knockdown A549 cells exhibited higher IFN-α, IFN-β, and IFN-λ1 mRNA levels following SeV stimulation compared with the control cells (Fig. 4C). We next restored the TAP1 production in TAP1-knockdown A549 cells by transfecting them with a TAP1 expression plasmid. Interestingly, restoration of TAP1 in the TAP1-KD cells reversed the increased mRNA levels of IFN-α, IFN-β, and IFN-λ1 (Fig. 4D), which indicated that the TAP1 depletion in TAP1-KD cells was responsible for the enhanced expression of the IFNs. Additionally, following SeV stimulation, the TAP1-KD A549 cells displayed higher expression levels of the ISGs, including Mx1, PKR, and OAS1, at both the mRNA (Fig. 4E) and protein levels (Fig. 4F). Additionally, we measured the induction of the IFNs and ISGs in TAP1-KD THP-1 cells in response to VSV infection, and the results were consistent with data observed in the TAP1-KD A549 cells (Fig. 4G, 4H). Thus, these results revealed that the endogenous TAP1 negatively regulates the virus-induced production of the IFNs and ISGs.

TAP1 is a negative regulator of virus-induced proinflammatory cytokines

Because our data indicated that TAP1 could attenuate the virus-triggered activation of IFN through NF-κB signaling, we further evaluated the expression of various NF-κB–responsive genes encoding proinflammatory cytokines such as IL-6, IL-8, IL-1β, and TNF-α. The qRT-PCR results showed that overexpression of TAP1 in A549 cells downregulated the SeV-induced proinflammatory cytokine expression at the mRNA level (Fig. 5A). To further confirm the potential role of the endogenous TAP1 in this process, we determined the mRNA levels of IL-6, IL-8, IL-1β, and TNF-α in TAP1-KD A549 cells infected with SeV (MOI of 1). The results showed that TAP1 depletion increased the mRNA levels of IL-6, IL-8, IL-1β, and TNF-α in response to SeV stimulation (Fig. 5B). However, the increased expression of IL-6, IL-8, IL-1β, and TNF-α in TAP1-KD A549 cells was inhibited when TAP1 was ectopically overexpressed (Fig. 5C). These data indicated that the TAP1 depletion in the TAP1-KD cells was responsible for the enhanced expression of these proinflammatory cytokines. Similarly, we also observed enhanced induction of IL-6, IL-8, IL-1β, and TNF-α in the TAP1-KD THP-1 cells infected with VSV (MOI of 1) (Fig. 5D). Subsequently, we assessed the effect of TAP1 on the activation of the IL-6 and IL-8 promoters following virus infection. The results showed that overexpression of TAP1 inhibited the SeV-triggered activation of the IL-6 and IL-8 promoters in A549 cells (Supplemental Fig. 1A), whereas knockdown of TAP1 had the opposite effect (Supplemental Fig. 1B). Taken together, these data indicated that TAP1 is a negative regulator of virus-induced production of proinflammatory cytokines.

TAP1 targets the TAK1 complex

On the basis of the results that TAP1 inhibited the virus-triggered activation of NF-κB but not ISRE, we proposed that TAP1 may be associated with components involved in the virus-triggered NF-κB signaling pathways. To evaluate the crosstalk between TAP1 and NF-κB signaling, we examined the effect of overexpression of TAP1 on the activation of NF-κB by cotransfecting the *NF-κB* lu-

shRNAs. A549 cells were transfected with the indicated RNAi plasmids for 36 h. The total RNA was isolated for qRT-PCR analysis, and the cell lysates were subjected to immunoblotting (left panel). HEK293T cells were transfected with the TAP1 and TRAF3 expression plasmids together with the indicated RNAi plasmids for 36 h. The cells were lysed and analyzed by immunoblotting with indicated Abs. TRAF3 was used as a reference for transfection (right panel). (**F**) A549 cells were transfected with shRNA-Scr. or shRNA-TAP1 for 24 h. The cells were harvested 24 h postinfection with IAV (MOI of 1). The relative levels of NP-specific mRNA, cRNA, and vRNA were measured using qRT-PCR. The TAP1 protein level was analyzed using immunoblotting. (**G**) RD cells were transfected with shRNA-Scr. or shRNA-TAP1 for 24 h. As in (D), cells were infected with EV71 (MOI of 1) and harvested 24 h postinfection. The intracellular levels of the vRNA and VP1 protein were detected using qRT-PCR and immunoblotting. (**H**) TAP1 induction in stable TAP1-knockdown A549 cells following IAV infection. The stable TAP1-KD A549 cells and control cells (Scr.-KD) were infected with IAV (MOI of 1) for the indicated times. The total RNA was isolated, and the TAP1 mRNA levels were examined using qRT-PCR. (**I**) The same numbers of TAP1-KD and Scr.-KD A549 cells were transfected with the vector or the TAP1 expression plasmids for 24 h. The cells were harvested 24 h after IAV infection (MOI of 1), and the relative levels of NP-specific mRNA, cRNA, and vRNA were measured using qRT-PCR. (**J**) Vero cells were transfected with the vector or the TAP1 expression plasmids for 24 h and then infected with VSV (MOI of 1). The VSV production in the supernatants was estimated as in (B). The TAP1 protein level was analyzed using immunoblotting. The graphs show the means ± SD, $n = 3$. $^{**}p < 0.01$. ND, not detected; Scr., scramble.

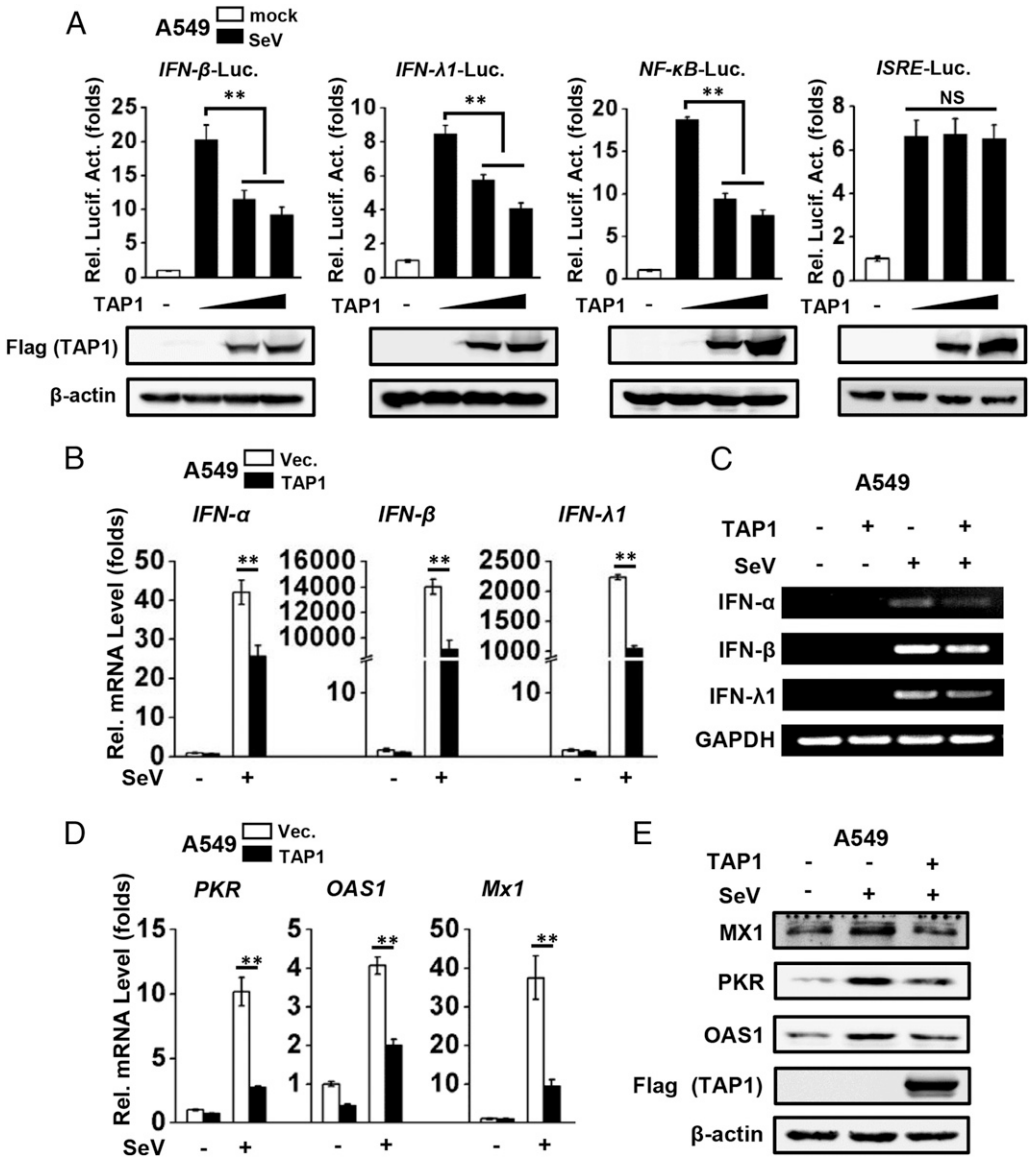

FIGURE 3. TAP1 suppressed the virus-triggered induction of IFNs and ISGs. (**A**) A549 cells were transfected with the indicated reporter plasmid (150 ng each), together with empty vector (no wedge) or increasing amounts of the TAP1 expression plasmid (wedge; 0, 150, or 300 ng) for 24 h, and then mock infected or infected with SeV (MOI of 1) for 12 h before the luciferase assays were performed. pRL-TK (150 ng) was cotransfected as an internal control. The results are presented relative to the *Renilla* luciferase activity. The levels of overexpressed TAP1 protein were determined by immunoblotting. (**B** and **C**) A549 cells were transfected with the vector or the TAP1 expression plasmid for 24 h and then mock infected or infected with SeV (MOI of 1) for 8 h. The total RNA was isolated, and the IFN mRNA levels were measured using qRT-PCR (B) and semiquantitative RT-PCR (C). (**D** and **E**) A549 cells were transfected with the vector or the TAP1 expression plasmid for 24 h and then mock infected or infected with SeV (MOI of 1) for 12 h. The mRNA (D) and protein (E) levels of PKR, OAS1, and Mx1 were determined using qRT-PCR and immunoblotting, respectively. The graphs show the means ± SD, $n = 3$. $^{**}p < 0.01$.

ciferase reporter plasmid and the TAP1 expression plasmid together with the indicated signaling molecules. The results demonstrated that expression of TAP1 inhibited the TRIF-, IRAK4-, RIG-I–, MAVS-, TRAF6-, and TAK1-triggered activation of NF-κB in a dose-dependent manner, but minimally affected the IKKα-, IKKβ-, p50-, or p65-triggered activation of NF-κB (Fig. 6A). These observations indicated that TAP1 may function immediately upstream of IKK complex, most likely at the level of TAK1. Subsequently, we performed coimmunoprecipitation assays in HEK293T cells to investigate the interaction between TAP1 and TAK1-associated components or other molecules involved. We found that TAP1 was associated with TAK1 and TAK1-TAB1 but not with any of the other examined components, including IRAK4, RIG-I, MAVS, IKKα, IκBα, p50, TRAF6, TBK1, and IKKβ (Fig. 6B, 6C). The interaction between TAP1 and TAK1 was confirmed by reciprocal coimmunoprecipitation experiments, in which RIG-I and TBK1 served as negative controls (Fig. 6D, 6E). Moreover, we sought to elucidate the relationship between TAP1 and other two TABs, TAB2 and TAB3. The results demonstrated that TAP1 was also associated with these two components of the TAK1 complex (Fig. 6F). Taken together, these results provided evidence that TAP1 constrained the virus-triggered innate immune response, possibly by targeting the TAK1–TAB1/2/3 complex.

Endogenous TAP1 interacts with TAK1

Because the knockdown of TAP1 enhanced the virus-triggered expression of the IFNs, ISGs, and proinflammatory cytokines in both A549 and THP-1 cells, we determined whether endogenous TAP1 was associated with TAK1 in these cells. The expression of TAP1 was induced in A549 cells by SeV infection for 0, 2, 12, and

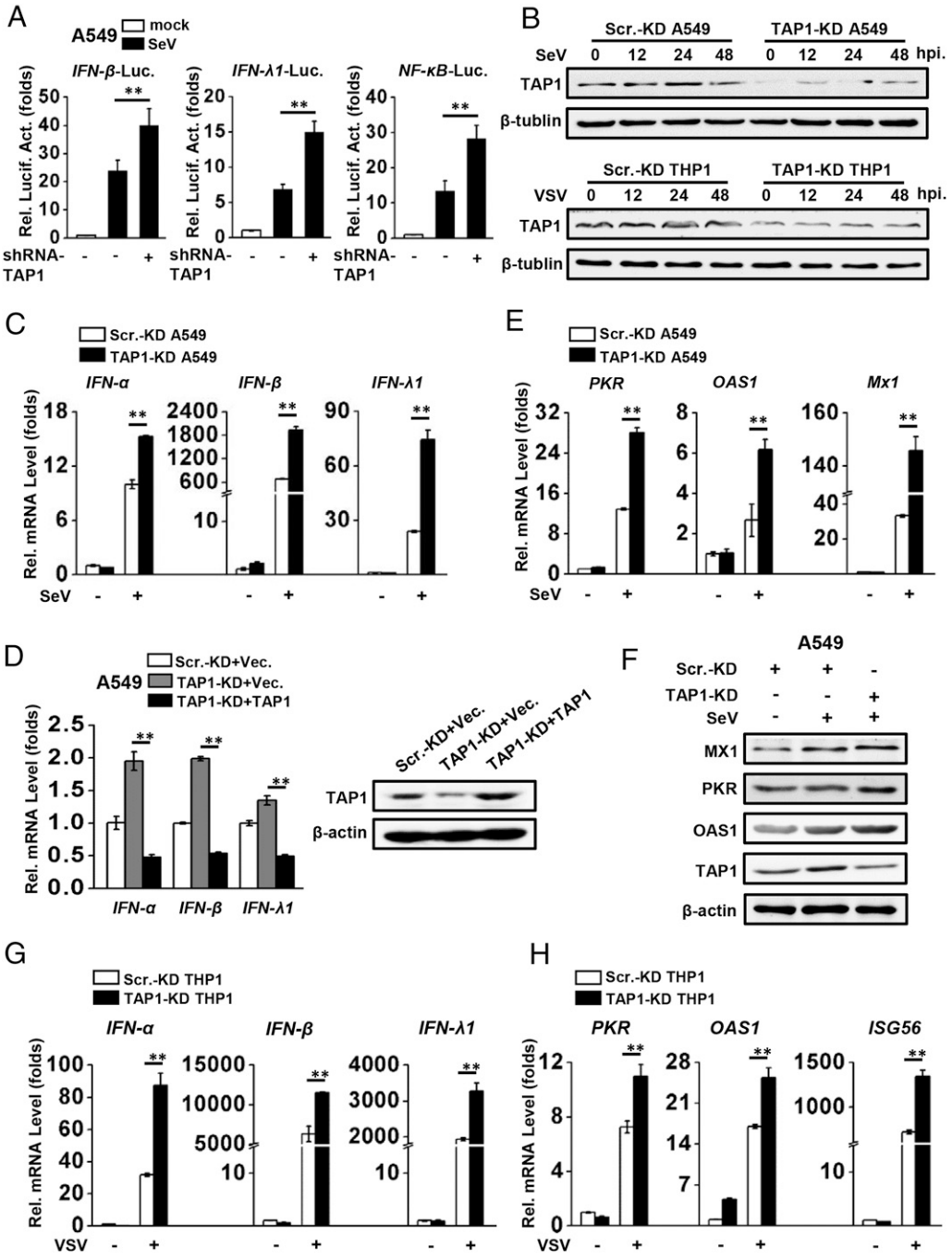

FIGURE 4. Knockdown of TAP1 enhances virus-triggered induction of IFNs and ISGs. (**A**) A549 cells were transfected with the indicated reporter plasmid (100 ng each), together with shRNA-scramble or shRNA-TAP1 (400 ng) for 24 h, and then mock infected or infected with SeV (MOI of 1) for 12 h before the luciferase assays were performed. pRL-TK (100 ng) was cotransfected as an internal control. The results are presented relative to the *Renilla* luciferase activity. (**B**) TAP1 induction in stable TAP1-KD cells following virus infection. The stable TAP1-KD A549 cells and the control cells (Scr.-KD) were infected with SeV (MOI of 1) for the indicated times, followed by immunoblot analysis (upper panel). The stable TAP1-KD THP-1 monocytes and control cells (Scr.-KD) were infected with VSV (MOI of 1) for the indicated times, followed by immunoblot analysis (lower panel). (**C**) TAP1-KD and Scr.-KD A549 cells were infected with SeV (MOI of 1) for 8 h before qRT-PCR. (**D**) The same numbers of TAP1-KD and Scr.-KD A549 cells were transfected with the vector or the TAP1 expression plasmid for 24 h followed by SeV infection (MOI of 1) for 8 h before the qRT-PCR was performed. The TAP1 protein levels were analyzed by immunoblotting. (**E** and **F**) TAP1-KD and Scr.-KD A549 cells were infected with SeV (MOI of 1) for 12 h. PKR, OAS1, and Mx1 mRNA (E) and protein (F) levels were determined by qRT-PCR and immunoblotting, respectively. (**G** and **H**) TAP1-KD and Scr.-KD THP-1 monocytes were infected with VSV (MOI of 1) for 8 h before the IFN mRNA levels were determined (G) or 12 h before the ISG mRNA levels were determined (H). The graphs show the means ± SD, $n = 3$. $^{**}p < 0.01$. Scr., scramble.

24 h, and then we performed coimmunoprecipitation experiments. The results suggested that endogenous TAP1 induced by viral infection was associated with endogenous TAK1 (Fig. 7A). In the THP-1 monocytes infected with VSV, similar interaction patterns were observed. In this experiment, TAP1 was not associated with TRAF6, which functions upstream of TAK1 (Fig. 7B). These data suggested that endogenous TAP1 was induced by viral infection and physically associated with TAK1. Previously, TAP1 has been reported to localize at the ER, whereas the TAK1 complex is thought to reside in cytosol. We wondered whether virus infec-

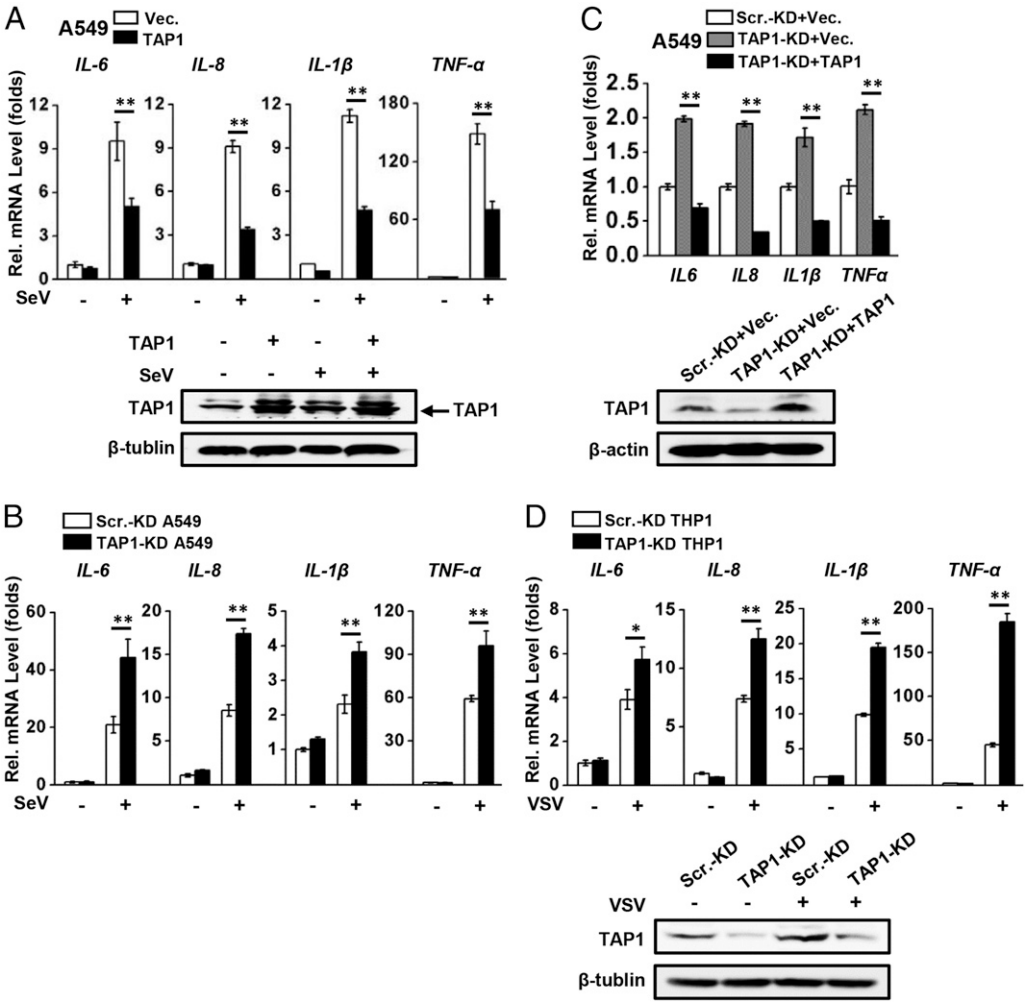

FIGURE 5. Identification of TAP1 as a negative regulator of virus-induced proinflammatory cytokines. (**A**) A549 cells were transfected with the vector or the TAP1 expression plasmid for 24 h followed by SeV infection (MOI of 1) for 12 h. The IL-6, IL-8, IL-1β, and TNF-α mRNA levels were measured using qRT-PCR. The TAP1 protein levels were analyzed by immunoblotting. (**B**) The same numbers of TAP1-KD and Scr.-KD A549 cells were mock infected or infected with SeV (MOI of 1) for 12 h followed by qRT-PCR. (**C**) The TAP1-KD and Scr.-KD A549 cells were transfected with the vector or the TAP1 expression plasmid for 24 h and then infected with SeV (MOI of 1) for 12 h followed by qRT-PCR and immunoblot analysis. (**D**) The same numbers of TAP1-KD and Scr.-KD THP-1 cells were mock infected or infected with VSV (MOI of 1) for 12 h followed by qRT-PCR. The TAP1 protein levels were analyzed using immunoblotting. The graphs show the means ± SD, $n = 3$. $^{*}p < 0.05$, $^{**}p < 0.01$. Scr., scramble.

tion affected the subcellular localization of TAP1. As shown by subcellular fractionation experiments, most of the TAP1 was localized in ER-containing membrane fractions but was minimally present in cytosol. This localization was not affected following SeV infection, although the overall expression of TAP1 was elevated (Fig. 7C). Accordingly, the confocal microscopy data showed that TAP1 was closely colocalized with the ER marker molecule GRP78 in both mock-infected and SeV-infected A549 cells (Fig. 7D). Based on these data, we proposed that the inducible ER-associated TAP1 was associated with cytosolic TAK1.

TAP1 inhibits virus-triggered NF-κB activation by affecting TAK1 phosphorylation

Our results showed that the TAP1 targeted the TAK1 complex and interfered with the virus-induced NF-κB activation. We next examined the effect of TAP1 on the virus-triggered NF-κB translocation and its upstream events, including IKK and IκBα phosphorylation. The results showed that TAP1 expression significantly inhibited the IKK and IκBα phosphorylation in A549 cells stimulated with SeV (Fig. 8A, 8B). The nuclear extraction experiments revealed that TAP1 expression clearly reduced the SeV-triggered translocation of the NF-κB subunits p50 and p65 from the cytosol to the nucleus (Fig. 8C), whereas the total protein levels of p65 and p50 were not affected (Fig. 8D). Additionally, we observed increased translocation of NF-κB into the nucleus in the TAP1-KD A549 cells (Fig. 8E). This effect of TAP1 on NF-κB translocation was confirmed by immunofluorescence microscopy (Fig. 8F, 8G). We further explored how TAP1 interfered with the virus-triggered TAK1-mediated signaling. Because our results demonstrated that TAP1 interacted with TAK1 and TABs, including TAB1, TAB2, and TAB3, we sought to determine whether TAP1 influenced the TAK1 phosphorylation, which is crucial for TAK1 activation and is facilitated by the TABs (52–54). The results indicated that overexpression of TAP1 reduced the virus triggered phosphorylation of TAK1 (Fig. 8H). Knockdown of TAP1 using siRNA increased the phosphorylation of TAK1 at 4 h after SeV infection (Fig. 8I). These findings were consistent and indicated that TAP1 impairs the virus-triggered NF-κB activation by targeting the TAK1 complex and hampering the phosphorylation of TAK1 (Fig. 9).

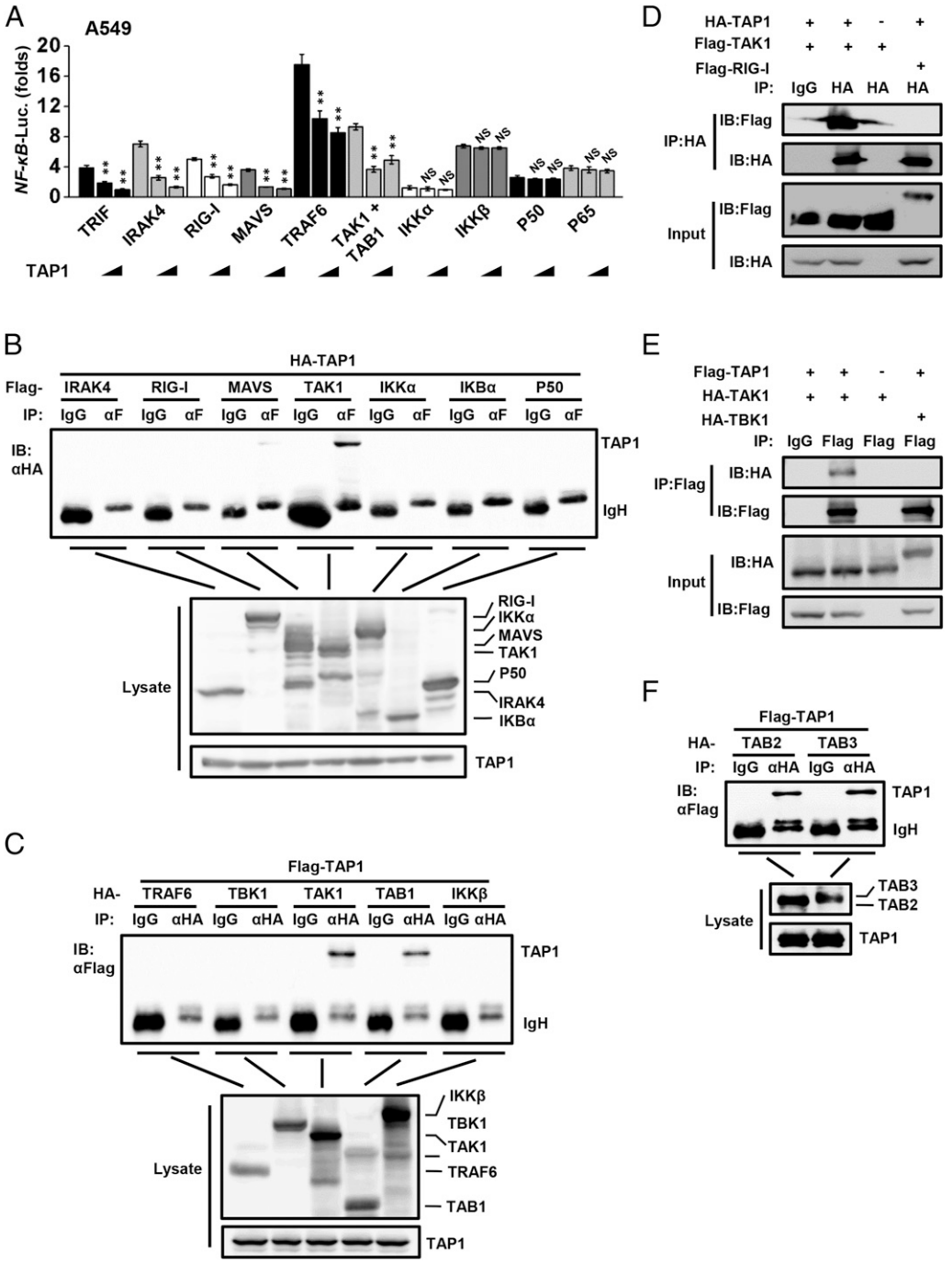

FIGURE 6. TAP1 targets the TAK1 complex. (**A**) A549 cells were transfected with the NF-κB luciferase reporter plasmid (100 ng) and the indicated expression plasmids (200 ng), along with empty vector (no wedge) or with increasing amounts (wedge; 100 and 200 ng) of the TAP1 expression plasmid for 24 h followed by VSV infection (MOI of 1) for another 12 h before the NF-κB luciferase assays were performed. pRL-TK (100 ng) was cotransfected as an internal control. The results are presented relative to the *Renilla* luciferase activity. $^{**}p < 0.01$. (**B**–**F**) TAP1 interacts with the TAK1–TAB1/2/3 complex. HEK293T cells were transfected with the indicated plasmids for 36 h. Coimmunoprecipitation and immunoblotting were performed with the indicated Abs. Flag-tagged TAK1 interacted with the HA-tagged TAP1 (B), HA-tagged TAK1 and TAB1 interacted with the Flag-tagged TAP1 (C), HA-tagged TAP1 interacted with the Flag-tagged TAK1 (D), Flag-tagged TAP1 interacted with the HA-tagged TAK1 (E), and HA-tagged TAB2 and TAB3 interacted with the Flag-tagged TAP1 (F). The data are from one of three experiments with similar results.

Discussion

Currently, two reports have shown that viral infections induce TAP1 expression (55, 56). One study employed DNA microarray technology to describe the changes in liver gene expression during the course of an acute-resolving HCV infection in a chimpanzee. TAP1 was one of genes upregulated in the liver during the acute HCV infection (55). The other study used a quantitative proteomic analysis to identify proteins that are potentially involved in innate immunity. The TAP1 protein was induced in SeV-infected HepG2 cells compared with uninfected cells (56). In the present study, we examined the TAP1 mRNA and protein levels in A549 cells infected with IAV and found that the TAP1 expression was upregulated in a time-dependent manner during the IAV replication (Fig. 1A). In THP-1 monocytes, IAV and VSV infections also induced TAP1 expression (Fig. 1B). Further investigation showed that IAV and SeV induced the activity of the *TAP1* promoter

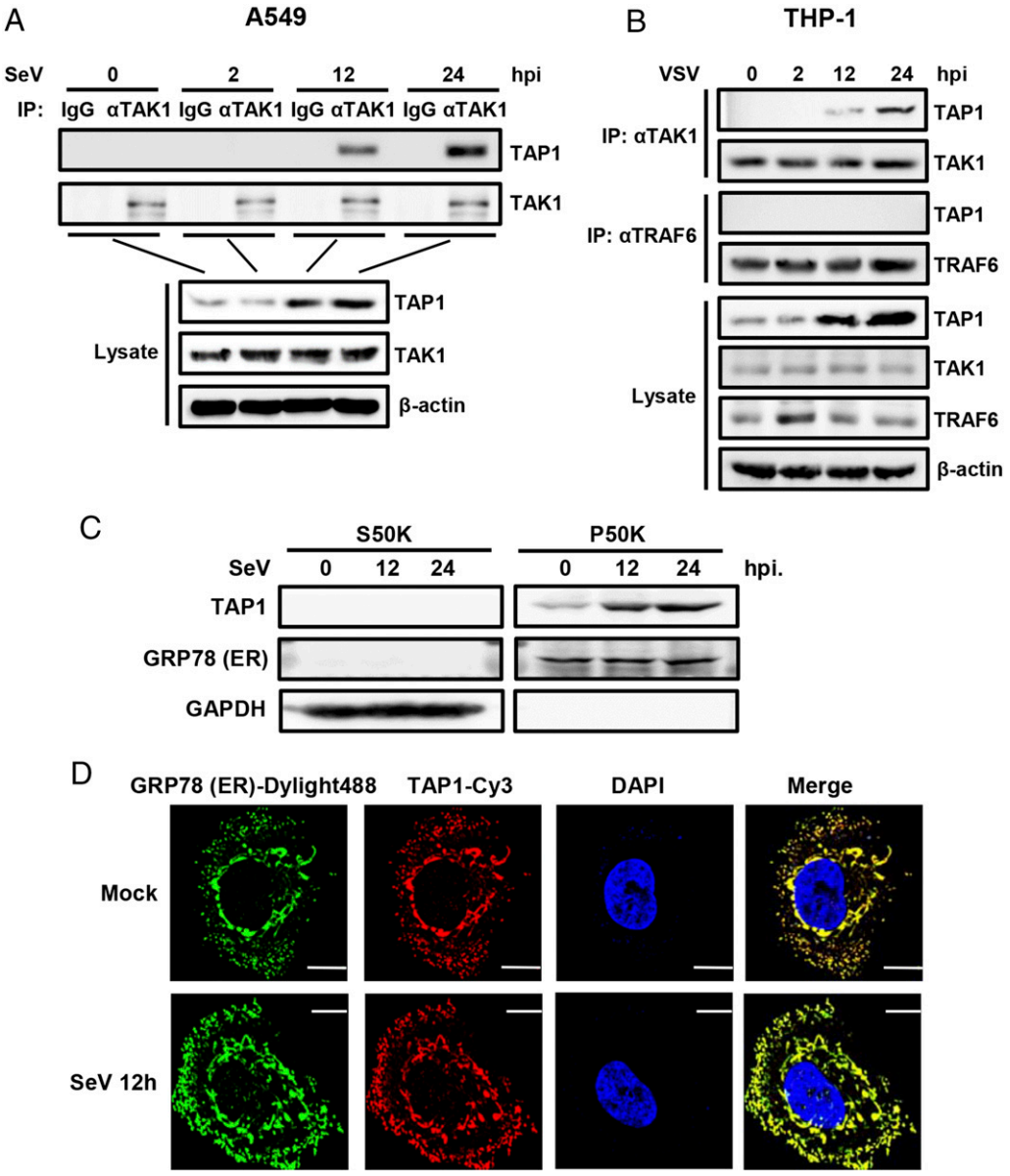

FIGURE 7. Endogenous TAP1 interacts with TAK1. (**A**) A549 cells were mock infected or infected with SeV (MOI of 1) for the indicated times. Coimmunoprecipitation and immunoblot analyses were performed with the indicated Abs. (**B**) THP-1 cells were mock infected or infected with VSV (MOI of 1) for the indicated times. Coimmunoprecipitation and immunoblot analyses were performed with the indicated Abs. (**C**) A549 cells were mock infected or infected with SeV (MOI of 1) for the indicated times. The cytosolic fractions (S50K) and the ER-containing membrane fractions (P50K) were separated using a subcellular fractionation method and analyzed by immunoblotting with the indicated Abs. GAPDH and GRP78 were used as the cytosolic and ER markers, respectively. (**D**) A549 cells were mock infected or infected with SeV (MOI of 1) for 12 h. GRP78 (ER)/TAP1 and the nuclei were stained with DyLight 488/Cy3–conjugated secondary Abs and DAPI, respectively, before observation using confocal microscopy. Scale bars, 10 μm. The data are from one of three experiments with similar results.

(Fig. 1D). Interestingly, the upregulation of TAP1 by virus infection was not dependent on IFN but was caused by virus itself (Fig. 1E, 1F). Previous studies reported that TAP1 could be induced by IFNs (46, 48, 49). It seems that TAP1 is a gene whose expression can be induced by both virus infection and IFNs. Based on these observations, we subsequently sought to explore whether TAP1 had any effect on the outcome of virus infections in cell cultures. The results from several virus infection systems indicated that the virus-inducible TAP1 subsequently promoted the replication of IAV, VSV, and EV71 (Fig. 2A–I). The observation that VSV replication was not affected by TAP1 in Vero cells (Fig. 2J) implied that the function of TAP1 in the promotion of virus replication may be associated with IFN signaling. Additionally, we have tested the effect of TAP1 on VSV replication in other cell types, including HeLa, Huh7, A549 IFNAR1-KO, and Huh7 IFNAR1-KO cells. The results showed that TAP1 overexpression enhanced VSV replication in HeLa (Supplemental Fig. 2A) and Huh7 (Supplemental Fig. 2B) cells, which were consistent with our findings in A549 cells. Moreover, we employed A549 IFNAR1-KO (Supplemental Fig. 2C) and Huh7 IFNAR1-KO cells (Supplemental Fig. 2D) to explore the relationship between IFN signaling and TAP1-mediated increase of virus replication. The results showed that in IFNAR1-KO cells, TAP1 overexpression had no effect on VSV replication (Supplemental Fig. 2E, 2F). These data further confirmed that TAP1 facilitates VSV replication by affecting IFN-dependent antiviral response. To date, except for the viral inhibition of TAP for immune evasion, other roles for TAP1 in the host–virus interaction have not been

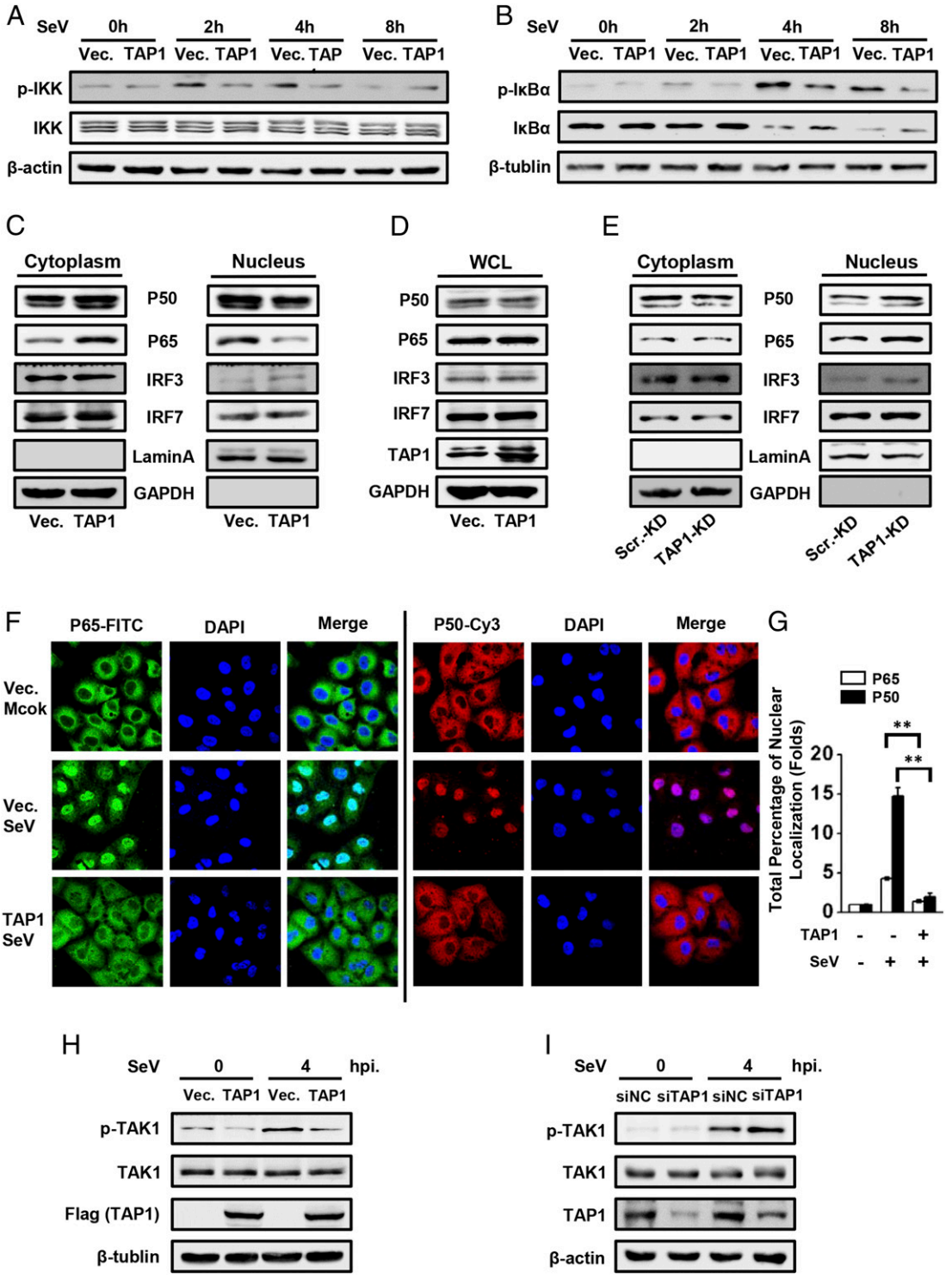

FIGURE 8. TAP1 inhibits virus-triggered NF-κB activation by hampering TAK1 phosphorylation. (**A** and **B**) TAP1 suppressed the virus-triggered phosphorylation of IKK and IκBα. A549 cells were transfected with the empty vector or the TAP1 expression plasmid for 24 h, then infected with SeV (MOI of 1) for the indicated times, followed by immunoblotting with the indicated Abs. (**C**–**G**) TAP1 impaired NF-κB translocation from the cytoplasm into the nucleus. (C) A549 cells were transfected with the empty vector or the TAP1 expression plasmid for 24 h, then infected with SeV (MOI of 1) for 12 h. The cytosolic and nuclear extracts were prepared for immunoblotting. GAPDH and LaminA were used as cytosolic and nuclear markers, respectively. (D) A549 cells were transfected with the empty vector or the TAP1 expression plasmid for 24 h, then infected with SeV (MOI of 1) for 12 h. The whole-cell lysates were analyzed by immunoblotting with the indicated Abs. (E) TAP1-KD and Scr.-KD A549 cells were infected with SeV (MOI of 1) for 12 h. The cytosolic and nuclear extracts were prepared for immunoblotting. (F) A549 cells were transfected with the vector or the TAP1 expression plasmid for 24 h, then mock infected or infected with SeV (MOI of 1) for 12 h. After fixation and permeabilization, the cells were immunostained with the indicated Abs and the nuclei were stained with DAPI. Original magnification ×60. (G) The total percentage of p50 and p65 nuclear localization was quantified using ImageJ software; each column represents the average of all the cells in the corresponding group in (F), and error bars represent the SEM. Results are presented relative to the results obtained from control group with the value set as 1. $^{**}p < 0.01$. (**H** and **I**) TAP1 affected the phosphorylation of TAK1. A549 cells were transfected with the indicated expression plasmids (H) or siRNAs (I) for 24 h, then mock infected or infected with SeV (MOI of 1) for 4 h, followed by immunoblotting with the indicated Abs. The data are from one of three experiments with similar results. Scr., scramble.

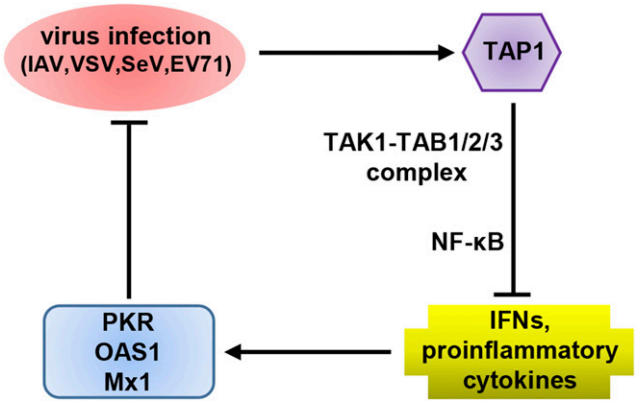

FIGURE 9. A hypothetical model for TAP1 function in virus-triggered innate immunity. Viruses induce TAP1 expression. In turn, TAP1 suppresses the endogenous IFNs, proinflammatory cytokines, and ISGs production by blocking NF-κB signaling by interacting with TAK1 complex and hampering TAK1 phosphorylation, ultimately resulting in enhanced virus replication.

established. In this study, we found that TAP1 enhanced viral replication in vitro, which was independent of the host adaptive immunity. This result implied a novel link between TAP1 and the innate immune response.

Our results showed that TAP1 had a significant influence on the activation of NF-κB but not that of IRF3/IRF7. Upon viral infection, PRRs initiate signaling cascades that lead to phosphorylation of the IKK complex and IκBα, the latter of which is subsequently ubiquitinated and degraded via the proteasome pathway. NF-κB is then released and translocates to the nucleus. Our results demonstrated that TAP1 inhibited the virus-induced IKK and IκBα phosphorylation and thus repressed the activation and nuclear translocation of NF-κB (Fig. 8), which led to impaired IFN expression and ISG production (Figs. 3, 4). These data at least partially explained the observation that TAP1 facilitated virus replication. Additionally, consistent with the results obtained from the *ISRE* reporter assay (Fig. 3A), TAP1 had no effect on the nuclear translocation of IRF3/IRF7 (Fig. 8C, 8E), which further confirmed that TAP1 only regulated NF-κB signaling. Our data revealed a previously undescribed function of TAP1 in the negative control of antiviral innate immunity.

Activation of NF-κB signaling also leads to the production of proinflammatory cytokines, including IL-6, IL-8, IL-1β, and TNF-α, which, in turn, promote the inflammatory response. Increasing evidence has indicated that dysregulated innate immunity may occur in many inflammation-associated diseases (57). Moreover, the proinflammatory cytokines produced by innate immune cells in chronic inflammatory conditions have been shown to play decisive roles in tumor development (57, 58). Although the acute inflammatory responses induced by viral infection are involved in host defense and viral clearance, excessive inflammation results in self-damage. Therefore, NF-κB needs to be tightly regulated through multiple negative regulators. In this study, we identified TAP1 as a negative regulator of the virus-triggered proinflammatory cytokine production. Consistent with the observation that TAP1 negatively regulated NF-κB activation, we found that ectopic expression of TAP1 suppressed the virus-triggered production of proinflammatory mediators, including IL-6, IL-8, IL-1β, and TNF-α (Fig. 5). Conversely, knockdown of TAP1 had the opposite effect (Fig. 5). Several regulatory proteins of the inflammatory process, including A20, CYLD, and the IκB family, are direct transcriptional targets of NF-κB and therefore form a negative feedback loop (59–61). Interestingly, previous studies showed that TAP1 is induced by IFNs and some TLR ligands in a cell type–specific manner (46–49). We observed a similar upregulation of TAP1 after virus infection. Thus, we hypothesized that TAP1 may mediate the crosstalk between NF-κB signaling and IFN downstream pathways in a feedback process to avoid excessive IFN production and inflammatory immune responses.

Further investigations indicated that TAP1 inhibited NF-κB signaling by targeting the TAK1 complex. Many regulatory molecules, including the phosphatase holoenzyme PP1, tripartite motif 8, and USP18, have been reported to target the TAK1–TAB complex to suppress NF-κB signaling (62–64). In this study, we demonstrated that TAP1 inhibited the NF-κB signaling by targeting the TAK1–TAB complex as indicated by the reporter assay–based screening and confirmed using coimmunoprecipitation (Figs. 6, 7). Moreover, TAP1 achieved this inhibitory effect on TAK1-mediated NF-κB signaling by blocking the phosphorylation of TAK1 (Fig. 8H, 8I). It has been reported that TAK1 phosphorylation is crucial for TAK1 activation and is facilitated by TABs (15, 52–54). We demonstrated that TAP1 interacted with TAK1 and TABs, including TAB1, TAB2, and TAB3. Therefore, we hypothesized that TAP1 blocks TAK1 phosphorylation probably by disrupting the association of TAK1 and TABs, which requires further investigations.

TAP1 is well known for its role in Ag presentation and adaptive immunity. Much progress has been made in understanding this process, but little is known about other functions of TAP1. In this study, our data, which were obtained from in vitro experiments, demonstrated the involvement of TAP1 in the negative control of virus-induced NF-κB signaling and the cellular antiviral response. Our results do not challenge the previously described role of TAP1 in Ag presentation. Actually, it is possible that these two opposing functions of TAP1 coexist in host innate and adaptive immunity. A previous study reported that the hepatitis B virus–induced calreticulin protein is involved in IFN resistance (65). Calreticulin enhances hepatitis B virus replication by suppressing IFN-α production and inhibiting the downstream antiviral effectors. Intriguingly, similar to TAP1, calreticulin is also an ER-associated protein and is well established to be an important participator in antigenic peptide processing and transport (66, 67). Another report indicated that two opposing functions of IKKβ were observed during acute and chronic intestinal inflammation (68).

Based on these data, we proposed a working model for the role of TAP1 in the negative regulation of virus-induced immune signaling (Fig. 9). In this model, viral infection induces TAP1 expression. TAP1 interacts with the TAK1–TAB complex and suppresses the TAK1 phosphorylation to block NF-κB signaling, which leads to a reduction in the production of the endogenous IFNs, proinflammatory cytokines, and ISGs. This, in turn, results in enhanced virus replication. For the viruses, TAP1 is an inducible host factor that facilitates viral replication. In the context of the host immune system, TAP1 is a negative regulator that helps to avoid excessive immune and inflammatory responses. Our research provides evidence for a novel role for TAP1 in the host–virus crosstalk.

Acknowledgments

We thank the Hongbing Shu laboratory at the College of Life Sciences of Wuhan University for supplying reporter plasmids, as well as the Yingliang Wu laboratory at the College of Life Sciences of Wuhan University for plasmids used in the construction of recombinant lentivirus.

Disclosures

The authors have no financial conflicts of interest.

References

1. Brennan, K., and A. G. Bowie. 2010. Activation of host pattern recognition receptors by viruses. *Curr. Opin. Microbiol.* 13: 503–507.
2. Akira, S., S. Uematsu, and O. Takeuchi. 2006. Pathogen recognition and innate immunity. *Cell* 124: 783–801.
3. Takeda, K., and S. Akira. 2004. TLR signaling pathways. *Semin. Immunol.* 16: 3–9.
4. Kawai, T., K. Takahashi, S. Sato, C. Coban, H. Kumar, H. Kato, K. J. Ishii, O. Takeuchi, and S. Akira. 2005. IPS-1, an adaptor triggering RIG-I- and Mda5-mediated type I interferon induction. *Nat. Immunol.* 6: 981–988.
5. Hiscott, J. 2007. Convergence of the NF-κB and IRF pathways in the regulation of the innate antiviral response. *Cytokine Growth Factor Rev.* 18: 483–490.
6. Stark, G. R., and J. E. Darnell, Jr. 2012. The JAK-STAT pathway at twenty. *Immunity* 36: 503–514.
7. Levy, D. E., and A. García-Sastre. 2001. The virus battles: IFN induction of the antiviral state and mechanisms of viral evasion. *Cytokine Growth Factor Rev.* 12: 143–156.
8. Schneider, W. M., M. D. Chevillotte, and C. M. Rice. 2014. Interferon-stimulated genes: a complex web of host defenses. *Annu. Rev. Immunol.* 32: 513–545.
9. Janeway Jr., C. A., and R. Medzhitov. 2002. Innate immune recognition. *Annu. Rev. Immunol.* 20: 197–216.
10. Seth, R. B., L. Sun, and Z. J. Chen. 2006. Antiviral innate immunity pathways. *Cell Res.* 16: 141–147.
11. Akira, S., K. Takeda, and T. Kaisho. 2001. Toll-like receptors: critical proteins linking innate and acquired immunity. *Nat. Immunol.* 2: 675–680.
12. Kawai, T., and S. Akira. 2011. Toll-like receptors and their crosstalk with other innate receptors in infection and immunity. *Immunity* 34: 637–650.
13. Skaug, B., X. Jiang, and Z. J. Chen. 2009. The role of ubiquitin in NF-κB regulatory pathways. *Annu. Rev. Biochem.* 78: 769–796.
14. Deng, L., C. Wang, E. Spencer, L. Yang, A. Braun, J. You, C. Slaughter, C. Pickart, and Z. J. Chen. 2000. Activation of the IkappaB kinase complex by TRAF6 requires a dimeric ubiquitin-conjugating enzyme complex and a unique polyubiquitin chain. *Cell* 103: 351–361.
15. Wang, C., L. Deng, M. Hong, G. R. Akkaraju, J. Inoue, and Z. J. Chen. 2001. TAK1 is a ubiquitin-dependent kinase of MKK and IKK. *Nature* 412: 346–351.
16. Fitzgerald, K. A., S. M. McWhirter, K. L. Faia, D. C. Rowe, E. Latz, D. T. Golenbock, A. J. Coyle, S. M. Liao, and T. Maniatis. 2003. IKKε and TBK1 are essential components of the IRF3 signaling pathway. *Nat. Immunol.* 4: 491–496.
17. Sharma, S., B. R. tenOever, N. Grandvaux, G. P. Zhou, R. Lin, and J. Hiscott. 2003. Triggering the interferon antiviral response through an IKK-related pathway. *Science* 300: 1148–1151.
18. Iwamura, T., M. Yoneyama, K. Yamaguchi, W. Suhara, W. Mori, K. Shiota, Y. Okabe, H. Namiki, and T. Fujita. 2001. Induction of IRF-3/-7 kinase and NF-κB in response to double-stranded RNA and virus infection: common and unique pathways. *Genes Cells* 6: 375–388.
19. Kawai, T., S. Sato, K. J. Ishii, C. Coban, H. Hemmi, M. Yamamoto, K. Terai, M. Matsuda, J. Inoue, S. Uematsu, et al. 2004. Interferon-α induction through Toll-like receptors involves a direct interaction of IRF7 with MyD88 and TRAF6. *Nat. Immunol.* 5: 1061–1068.
20. Honda, K., H. Yanai, T. Mizutani, H. Negishi, N. Shimada, N. Suzuki, Y. Ohba, A. Takaoka, W. C. Yeh, and T. Taniguchi. 2004. Role of a transductional-transcriptional processor complex involving MyD88 and IRF-7 in Toll-like receptor signaling. *Proc. Natl. Acad. Sci. USA* 101: 15416–15421.
21. Seth, R. B., L. Sun, C. K. Ea, and Z. J. Chen. 2005. Identification and characterization of MAVS, a mitochondrial antiviral signaling protein that activates NF-κB and IRF3. *Cell* 122: 669–682.
22. Xu, L. G., Y. Y. Wang, K. J. Han, L. Y. Li, Z. Zhai, and H. B. Shu. 2005. VISA is an adapter protein required for virus-triggered IFN-β signaling. *Mol. Cell* 19: 727–740.
23. Meylan, E., J. Curran, K. Hofmann, D. Moradpour, M. Binder, R. Bartenschlager, and J. Tschopp. 2005. Cardif is an adaptor protein in the RIG-I antiviral pathway and is targeted by hepatitis C virus. *Nature* 437: 1167–1172.
24. Mikkelsen, S. S., S. B. Jensen, S. Chiliveru, J. Melchjorsen, I. Julkunen, M. Gaestel, J. S. Arthur, R. A. Flavell, S. Ghosh, and S. R. Paludan. 2009. RIG-I-mediated activation of p38 MAPK is essential for viral induction of interferon and activation of dendritic cells: dependence on TRAF2 and TAK1. *J. Biol. Chem.* 284: 10774–10782.
25. Zhong, B., P. Tien, and H. B. Shu. 2006. Innate immune responses: crosstalk of signaling and regulation of gene transcription. *Virology* 352: 14–21.
26. Li, Q., and I. M. Verma. 2002. NF-κB regulation in the immune system. *Nat. Rev. Immunol.* 2: 725–734.
27. Häcker, H., and M. Karin. 2006. Regulation and function of IKK and IKK-related kinases. *Sci. STKE* 2006: re13.
28. Ajibade, A. A., H. Y. Wang, and R. F. Wang. 2013. Cell type-specific function of TAK1 in innate immune signaling. *Trends Immunol.* 34: 307–316.
29. Dai, L., C. Aye Thu, X. Y. Liu, J. Xi, and P. C. Cheung. 2012. TAK1, more than just innate immunity. *IUBMB Life* 64: 825–834.
30. Kelly, A., S. H. Powis, L. A. Kerr, I. Mockridge, T. Elliott, J. Bastin, B. Uchanska-Ziegler, A. Ziegler, J. Trowsdale, and A. Townsend. 1992. Assembly and function of the two ABC transporter proteins encoded in the human major histocompatibility complex. *Nature* 355: 641–644.
31. Spies, T., V. Cerundolo, M. Colonna, P. Cresswell, A. Townsend, and R. DeMars. 1992. Presentation of viral antigen by MHC class I molecules is dependent on a putative peptide transporter heterodimer. *Nature* 355: 644–646.
32. Spies, T., and R. DeMars. 1991. Restored expression of major histocompatibility class I molecules by gene transfer of a putative peptide transporter. *Nature* 351: 323–324.
33. Mayerhofer, P. U., and R. Tampé. 2015. Antigen translocation machineries in adaptive immunity and viral immune evasion. *J. Mol. Biol.* 427: 1102–1118.
34. Ressing, M. E., R. D. Luteijn, D. Horst, and E. J. Wiertz. 2013. Viral interference with antigen presentation: trapping TAP. *Mol. Immunol.* 55: 139–142.
35. Jun, Y., E. Kim, M. Jin, H. C. Sung, H. Han, D. E. Geraghty, and K. Ahn. 2000. Human cytomegalovirus gene products US3 and US6 down-regulate trophoblast class I MHC molecules. *J. Immunol.* 164: 805–811.
36. Dugan, G. E., and E. W. Hewitt. 2008. Structural and functional dissection of the human cytomegalovirus immune evasion protein US6. *J. Virol.* 82: 3271–3282.
37. Oldham, M. L., R. K. Hite, A. M. Steffen, E. Damko, Z. Li, T. Walz, and J. Chen. 2016. A mechanism of viral immune evasion revealed by cryo-EM analysis of the TAP transporter. *Nature* 529: 537–540.
38. Steer, H. J., R. A. Lake, A. K. Nowak, and B. W. Robinson. 2010. Harnessing the immune response to treat cancer. *Oncogene* 29: 6301–6313.
39. Wang, Q., X. Chen, J. Feng, Y. Cao, Y. Song, H. Wang, C. Zhu, S. Liu, and Y. Zhu. 2013. Soluble interleukin-6 receptor-mediated innate immune response to DNA and RNA viruses. *J. Virol.* 87: 11244–11254.
40. Li, Y., J. Xie, X. Xu, L. Liu, Y. Wan, Y. Liu, C. Zhu, and Y. Zhu. 2013. Inducible interleukin 32 (IL-32) exerts extensive antiviral function via selective stimulation of interferon λ1 (IFN-λ1). *J. Biol. Chem.* 288: 20927–20941.
41. Cao, Z., Y. Zhou, S. Zhu, J. Feng, X. Chen, S. Liu, N. Peng, X. Yang, G. Xu, and Y. Zhu. 2016. Pyruvate carboxylase activates the RIG-I-like receptor-mediated antiviral immune response by targeting the MAVS signalosome. *Sci. Rep.* 6: 22002.
42. Liu, S., N. Peng, J. Xie, Q. Hao, M. Zhang, Y. Zhang, Z. Xia, G. Xu, F. Zhao, Q. Wang, et al. 2015. Human hepatitis B virus surface and e antigens inhibit major vault protein signaling in interferon induction pathways. *J. Hepatol.* 62: 1015–1023.
43. Li, W., Y. Liu, M. M. Mukhtar, R. Gong, Y. Pan, S. T. Rasool, Y. Gao, L. Kang, Q. Hao, G. Peng, et al. 2008. Activation of interleukin-32 pro-inflammatory pathway in response to influenza A virus infection. *PLoS One* 3: e1985.
44. Mukhtar, M. M., S. Li, W. Li, T. Wan, Y. Mu, W. Wei, L. Kang, S. T. Rasool, Y. Xiao, Y. Zhu, and J. Wu. 2009. Single-chain intracellular antibodies inhibit influenza virus replication by disrupting interaction of proteins involved in viral replication and transcription. *Int. J. Biochem. Cell Biol.* 41: 554–560.
45. Peng, N., S. Liu, Z. Xia, S. Ren, J. Feng, M. Jing, X. Gao, E. A. Wiemer, and Y. Zhu. 2016. Inducible major vault protein plays a pivotal role in double-stranded RNA– or virus-induced proinflammatory response. *J. Immunol.* 196: 2753–2766.
46. Der, S. D., A. Zhou, B. R. Williams, and R. H. Silverman. 1998. Identification of genes differentially regulated by interferon α, β, or γ using oligonucleotide arrays. *Proc. Natl. Acad. Sci. USA* 95: 15623–15628.
47. Cecil, A. A., and M. J. Klemsz. 2004. p38 activation through Toll-like receptors modulates IFN-gamma-induced expression of the Tap-1 gene only in macrophages. *J. Leukoc. Biol.* 75: 560–568.
48. Cramer, L. A., S. L. Nelson, and M. J. Klemsz. 2000. Synergistic induction of the Tap-1 gene by IFN-γ and lipopolysaccharide in macrophages is regulated by STAT1. *J. Immunol.* 165: 3190–3197.
49. Min, W., J. S. Pober, and D. R. Johnson. 1998. Interferon induction of TAP1: the phosphatase SHP-1 regulates crossover between the IFN-α/β and the IFN-γ signal-transduction pathways. *Circ. Res.* 83: 815–823.
50. Prescott, J., P. Hall, M. Acuna-Retamar, C. Ye, M. G. Wathelet, H. Ebihara, H. Feldmann, and B. Hjelle. 2010. New World hantaviruses activate IFNλ production in type I IFN-deficient Vero E6 cells. *PLoS One* 5: e11159.
51. Pauli, E. K., M. Schmolke, T. Wolff, D. Viemann, J. Roth, J. G. Bode, and S. Ludwig. 2008. Influenza A virus inhibits type I IFN signaling via NF-κB-dependent induction of SOCS-3 expression. *PLoS Pathog.* 4: e1000196.
52. Ono, K., T. Ohtomo, S. Sato, Y. Sugamata, M. Suzuki, N. Hisamoto, J. Ninomiya-Tsuji, M. Tsuchiya, and K. Matsumoto. 2001. An evolutionarily conserved motif in the TAB1 C-terminal region is necessary for interaction with and activation of TAK1 MAPKKK. *J. Biol. Chem.* 276: 24396–24400.
53. Kishida, S., H. Sanjo, S. Akira, K. Matsumoto, and J. Ninomiya-Tsuji. 2005. TAK1-binding protein 2 facilitates ubiquitination of TRAF6 and assembly of TRAF6 with IKK in the IL-1 signaling pathway. *Genes Cells* 10: 447–454.
54. Kanayama, A., R. B. Seth, L. Sun, C. K. Ea, M. Hong, A. Shaito, Y. H. Chiu, L. Deng, and Z. J. Chen. 2004. TAB2 and TAB3 activate the NF-κB pathway through binding to polyubiquitin chains. *Mol. Cell* 15: 535–548.
55. Bigger, C. B., K. M. Brasky, and R. E. Lanford. 2001. DNA microarray analysis of chimpanzee liver during acute resolving hepatitis C virus infection. *J. Virol.* 75: 7059–7066.
56. Zhou, M. T., Y. Qin, M. Li, C. Chen, X. Chen, H. B. Shu, and L. Guo. 2015. Quantitative proteomics reveals the roles of peroxisome-associated proteins in antiviral innate immune responses. *Mol. Cell. Proteomics* 14: 2535–2549.
57. Takeuchi, O., and S. Akira. 2010. Pattern recognition receptors and inflammation. *Cell* 140: 805–820.
58. Karin, M. 2006. Nuclear factor-κB in cancer development and progression. *Nature* 441: 431–436.
59. Verhelst, K., I. Carpentier, M. Kreike, L. Meloni, L. Verstrepen, T. Kensche, I. Dikic, and R. Beyaert. 2012. A20 inhibits LUBAC-mediated NF-κB activation by binding linear polyubiquitin chains via its zinc finger 7. *EMBO J.* 31: 3845–3855.
60. Trompouki, E., E. Hatzivassiliou, T. Tsichritzis, H. Farmer, A. Ashworth, and G. Mosialos. 2003. CYLD is a deubiquitinating enzyme that negatively regulates NF-κB activation by TNFR family members. *Nature* 424: 793–796.

61. Komuro, A., D. Bamming, and C. M. Horvath. 2008. Negative regulation of cytoplasmic RNA-mediated antiviral signaling. *Cytokine* 43: 350–358.
62. Gu, M., C. Ouyang, W. Lin, T. Zhang, X. Cao, Z. Xia, and X. Wang. 2014. Phosphatase holoenzyme PP1/GADD34 negatively regulates TLR response by inhibiting TAK1 serine 412 phosphorylation. *J. Immunol.* 192: 2846–2856.
63. Liu, X., H. Li, B. Zhong, M. Blonska, S. Gorjestani, M. Yan, Q. Tian, D. E. Zhang, X. Lin, and C. Dong. 2013. USP18 inhibits NF-κB and NFAT activation during Th17 differentiation by deubiquitinating the TAK1–TAB1 complex. *J. Exp. Med.* 210: 1575–1590.
64. Shi, M., W. Deng, E. Bi, K. Mao, Y. Ji, G. Lin, X. Wu, Z. Tao, Z. Li, X. Cai, et al. 2008. TRIM30 alpha negatively regulates TLR-mediated NF-kappa B activation by targeting TAB2 and TAB3 for degradation. *Nat. Immunol.* 9: 369–377.
65. Yue, X., H. Wang, F. Zhao, S. Liu, J. Wu, W. Ren, and Y. Zhu. 2012. Hepatitis B virus-induced calreticulin protein is involved in IFN resistance. *J. Immunol.* 189: 279–286.
66. Sadasivan, B., P. J. Lehner, B. Ortmann, T. Spies, and P. Cresswell. 1996. Roles for calreticulin and a novel glycoprotein, tapasin, in the interaction of MHC class I molecules with TAP. *Immunity* 5: 103–114.
67. Liu, X., J. Li, Y. Liu, J. Ding, Z. Tong, Y. Liu, Y. Zhou, and Y. Liu. 2016. Calreticulin acts as an adjuvant to promote dendritic cell maturation and enhances antigen-specific cytotoxic T lymphocyte responses against non-small cell lung cancer cells. *Cell. Immunol.* 300: 46–53.
68. Eckmann, L., T. Nebelsiek, A. A. Fingerle, S. M. Dann, J. Mages, R. Lang, S. Robine, M. F. Kagnoff, R. M. Schmid, M. Karin, et al. 2008. Opposing functions of IKKβ during acute and chronic intestinal inflammation. *Proc. Natl. Acad. Sci. USA* 105: 15058–15063.